

## Air Force Institute of Technology AFIT Scholar

---

Theses and Dissertations

Student Graduate Works

---

6-17-2010

# Realistic Vertical Atmospheric Profiles and Effects from Limited Surface Observations

Dane P. Ranney

Follow this and additional works at: <https://scholar.afit.edu/etd>

 Part of the [Atmospheric Sciences Commons](#)

---

### Recommended Citation

Ranney, Dane P., "Realistic Vertical Atmospheric Profiles and Effects from Limited Surface Observations" (2010). *Theses and Dissertations*. 2173.  
<https://scholar.afit.edu/etd/2173>

This Thesis is brought to you for free and open access by the Student Graduate Works at AFIT Scholar. It has been accepted for inclusion in Theses and Dissertations by an authorized administrator of AFIT Scholar. For more information, please contact [richard.mansfield@afit.edu](mailto:richard.mansfield@afit.edu).



**REALISTIC VERTICAL ATMOSPHERIC PROFILES AND EFFECTS  
FROM LIMITED SURFACE OBSERVATIONS**

THESIS

Dane P. Ranney, CIV, USAF

AFIT/GAP/ENP/10-M12

**DEPARTMENT OF THE AIR FORCE  
AIR UNIVERSITY**

**AIR FORCE INSTITUTE OF TECHNOLOGY**

---

---

Wright-Patterson Air Force Base, Ohio

APPROVED FOR PUBLIC RELEASE; DISTRIBUTION UNLIMITED

The views expressed in this thesis are those of the author and do not reflect the official policy or position of the United States Air Force, Department of Defense, or the United States Government.

AFIT/GAP/ENP/10-M12

REALISTIC VERTICAL ATMOSPHERIC PROFILES AND EFFECTS  
FROM LIMITED SURFACE OBSERVATIONS

THESIS

Presented to the Faculty

Department of Engineering Physics

Graduate School of Engineering and Management

Air Force Institute of Technology

Air University

Air Education and Training Command

In Partial Fulfillment of the Requirements for the  
Degree of Master of Science in Engineering Physics

Dane P. Ranney, BS

Civilian, USAF

June 2010

APPROVED FOR PUBLIC RELEASE; DISTRIBUTION UNLIMITED.

AFIT/GAP/ENP/10-M12

REALISTIC VERTICAL ATMOSPHERIC PROFILES AND EFFECTS FROM  
LIMITED SURFACE OBSERVATIONS

Dane P. Ranney, BS

Civilian, USAF

Approved:

//SIGNED//  
Steven T. Fiorino, PhD (Chairman)

\_\_\_\_\_  
Date

//SIGNED//  
Lt Col Ariel O. Acebal (Member)

\_\_\_\_\_  
Date

//SIGNED//  
Kevin C. Gross, PhD (Member)

\_\_\_\_\_  
Date

### **Abstract**

The ability to accurately describe the atmospheric conditions around us is not only important to the Air Force, but to anyone involved in signal propagation. The programs currently utilized to describe the atmosphere take into account a variety of measures. The LEEDR (Laser Environmental Effects Definition and Reference) program in particular, allows the user to select a location, aerosol and molecular effects model, numerous cloud and precipitation events, as well as other features. Even with the control that the user has, the output that the program provides can vary from actual conditions on a day to day basis. This is due to LEEDR's dependence on averaged climatological data. In order to make the output more specific for deterministic conditions, two additions to the LEEDR program have been proposed. The incorporation of calculated or measured ground level characteristics will allow the program to extrapolate data from scenario-specific anchor points, leading to a more realistic depiction of conditions below the boundary layer for the scenario of interest. After making this modification to the LEEDR program, differences were observed in several of the output variables throughout the boundary layer. Also, after interpolating sounding data from a location near the LEEDR site to model ground level conditions, LEEDR was able to more accurately model upper air measurements. In addition, a Correlated-k band model has been developed to augment the line-by-line LEEDR calculation in order to reduce the computation time required to describe atmospheric transmission bands of the spectrum. This allows the implementation of fast calculating path radiance computations. As a stand-alone module, the Correlated-k method is able to calculate transmission for the band interval studied,

assuming a homogeneous atmosphere on average, 170% faster than the current transmission method in LEEDR.

## **Acknowledgments**

I would first like to sincerely thank my research advisor, Dr. Fiorino, for his support and guidance throughout my thesis quarters. Secondly, I would like to thank my committee members for their support in providing me with the knowledge necessary to reach my research goals. I would also like to thank Matthew Krizo for his help when I had questions concerning the LEEDR software. LEEDR consists of quite a few files, and his help in answering my questions was greatly appreciated. I would also like to thank Major Michael Saville for putting up with all my questions concerning how to program my Correlated-k database in MATLAB. Additionally, I would like to thank Lt Col John Dea and Lt Col Kyle Novak. Their vast mathematical knowledge helped me greatly throughout my project. Lastly, I would like to thank my family for instilling in me the strength necessary to finish this project.

Dane P. Ranney



# Table of Contents

	Page
Abstract.....	iv
Acknowledgments.....	vi
List of Figures.....	ix
List of Tables.....	xi
List of Acronyms.....	xii
I. Introduction.....	1
Motivation.....	1
Problem Statement.....	3
Approach.....	5
Document Outline.....	7
II. Literature Review.....	8
LEEDR (Laser Environmental Effects Definition and Reference).....	8
LEEDR (Absorption/Scattering).....	12
LEEDR (Turbulence Models).....	16
LBL (Line-By-Line Calculations).....	20
Band Models (Wide and Narrow Band Models).....	23
K-Distribution/Correlated-k.....	26
III. Methodology.....	30
Overview.....	30
User-Defined Ground Level Tab.....	30
Correlated-k Binning Method.....	34
IV. Analysis and Results.....	44
Overview.....	44
User-Defined Ground Level Input Tab.....	44
Correlated-k Algorithm Development.....	49
V. Conclusions and Recommendations.....	73
Overview.....	73
User-Defined Ground Level Input Tab.....	73
Correlated-k.....	73

	Page
Recommendations for Future Research .....	74
Appendix.....	76
Extinction Coefficient Database Source Code .....	76
Correlated-k Source Code .....	79
Bibliography.....	86

## List of Figures

Figure	Page
1. The ExPERT sites in LEEDR .....	9
2. Kolmogorov’s Model of Variation in the Atmosphere.....	19
3. User-Defined Ground Level GUI Tab Incorporated into LEEDR.....	31
4. User-Defined GUI Tab Safeguarding Technique .....	32
5. Illustration of the mapping of the absorption coefficient from the v- domain to the g-domain. (a) Absorption coefficients of three lines in the v-domain and division of the k-space into 10 equal intervals. The numbers are the data points in each interval with a total number of 35. (b) By definition, $g(j\Delta k) \equiv n(0, j\Delta k)/N$ , $j = 0, 1, \dots, 9$ . Thus, the data points in the v-domain are transformed to the g-domain, where g is a monotonic increasing function. (Courtesy of [9:134]) .....	36
6. Region of Low LEEDR Extinction.....	39
7. Correlated-k Transmission in a Region of Low LEEDR Extinction .....	40
8. Region of High LEEDR Extinction .....	41
9. Correlated-k Transmission in a Region of High LEEDR Extinction .....	41
10. Variation Observed in LEEDR Output Variables based on Ground Level Modification .....	48
11. LEEDR Extinction Coefficients Obtained for Correlated-k Process.....	51
12. Binned LEEDR Extinction Coefficients .....	52
13. Resulting k(g) Points for Correlated-k Method .....	53
14. Band-Averaged Correlated-k Transmittance for $4 \text{ cm}^{-1}$ Interval .....	54
15. Hypothetical Extinction Spectrum (Courtesy of Liou [9:134]) .....	56
16. Hypothetical k(g) Plot Produced from Correlated-k Script .....	57
17. Accuracy Comparison between Correlated-k and LEEDR Transmission.....	58

Figure	Page
18. Transmission Differences resulting from a Similar Correlated-k and LEEDR Run-time .....	59
19. Transmission Values for LEEDR, Correlated-k, Correlated-k (with LBLRTM), and Plexus from 13123 cm <sup>-1</sup> to 13167 cm <sup>-1</sup> .....	60
20. Correlated-k Transmission with Varying Bin Numbers .....	61
21. LEEDR Transmission Running Means with Correlated-k Transmission.....	63
22. Average LEEDR Extinction from 13123 cm <sup>-1</sup> to 13127 cm <sup>-1</sup> .....	65
23. Average Correlated-k Extinction from 13123 cm <sup>-1</sup> to 13127 cm <sup>-1</sup> .....	66
24. Average LEEDR and Correlated-k Extinction from 13123 cm <sup>-1</sup> to 13127 cm <sup>-1</sup> .....	67

## List of Tables

Table	Page
1. LEEDR Data without Ground level Modification .....	46
2. LEEDR Defined Atmosphere for Correlated-k Method .....	49
3. Correlated-k Run Times to Compile Extinction Coefficient Database .....	69
4. Correlated-k Run Times to Produce k(g) Database .....	69
5. Correlated-k Transmission File Run Times .....	70
6. Correlated-k Transmission Computation Times .....	71
7. LEEDR Run Times for Comparable Transmission Resolution to Correlated-k .....	71
8. LEEDR Run Times Used to Display Transmission Accuracy Loss to Correlated-k .....	72

## List of Acronyms

SPAWAR	Space and Naval Warfare Systems Command
AFIT	Air Force Institute of Technology
HELEEOS	High Energy Laser End-to-End Operational Simulation
ANAM	Advanced Navy Aerosol Model
GADS	Global Aerosol Dataset
NAAPS	Navy Aerosol Analysis and Prediction System
FAROP	Forecast of Aerosol Radiative and Optical Properties
AOD	Aerosol Optical Depth
SDL	Space Dynamics Laboratory
LEEDR	Laser Environmental Effects Definition and Reference
LBL	Line-by-Line
ExPERT	Extreme and Percentile Environmental Reference Tables
HITRAN	High-Resolution Transmission Molecular Absorption Database
MODTRAN	Moderate Spectral Resolution Atmospheric Transmission
HV 5/7	Huffnagel-Valley 5/7
CLEAR 1	Critical Laser Enhancing Atmospheric Research
SOR	Starfire Optical Range
NSLOT	Navy Surface Layer Optical Turbulence
GUI	Graphical User Interface
LUT	Lookup Table
AFRL	Air Force Research Lab

# REALISTIC VERTICAL ATMOSPHERIC PROFILES AND EFFECTS FROM LIMITED SURFACE OBSERVATIONS

## I. Introduction

### Motivation

The ability to accurately describe our atmosphere is extremely important in terms of our ability to analyze electromagnetic wave propagation. In terms of signal and image analysis in particular, our ability to accurately perform both types of analyses ultimately depends on conditions in the atmosphere. Most current radiative transfer programs that are used to perform image and signal analysis however, rely on a database of climatologically averaged data. Thus, atmospheric quantities, such as dewpoint, temperature, and aerosol concentration, which depend on a certain hour of the day, are taken from a database that averages the data based on previously recorded observations.

In addition to the previous problem, another problem exists with respect to the calculation time that most atmospheric programs use to compute transmission. After the user has specified the characteristics of the atmosphere, as well as the part of the domain, most programs (radiative transfer codes) utilize a calculation technique which determines the extinction (how much radiation is scattered or absorbed along the user's path) in radiation at several points along the path. Thus, at the end of the user's path length, a discretely sampled estimation of the extinction in the radiation is presented to the user. As one would suspect, for a very detailed program, this could become very computationally expensive. The ability to obtain signal or image analysis in a timely manner could certainly prove to be very beneficial. A faster calculation algorithm could be implemented to improve upon remote sensing and spectroscopy applications [12].

From a community based standpoint, one example that relates to the previous discussion is the research currently being conducted between the Navy SPAWAR (Space and Naval Warfare Systems Command) and AFIT (Air Force Institute of Technology). On June 24, 2009, a representative of the Navy SPAWAR gave a talk concerning their ability to accurately predict communication and image capabilities under varying ocean atmosphere conditions. The talk focused on tests that were conducted at Eglin Air Force Base, utilizing an atmospheric package called HELEEOS (High Energy Laser End-to-End Operational Simulation). The HELEEOS program, in summary, allows the user to perform path radiance calculations with respect to radiation of a user-defined wavelength (from the visible to far-infrared). The user has control over numerous features of the atmosphere, as well as the target (receiving the radiation), platform (emitting the radiation), and observer. Applications of this program include: remote sensing and signal analysis capabilities. In response to the tests however, the Navy SPAWAR noticed that on certain timescales, there was more or less signal degradation than what was accounted for by HELEEOS (HELEEOS profile used in these tests is described in more detail in [6]). Thus, a project was proposed, to build an additional atmospheric profile in HELEEOS in order to enable the user to have more control over describing their environment. The project, as outlined, would essentially encompass various point-based and field-based methodologies. The field-based models and measurements would include “local (shipboard) meteorology, surface meteorology stations, radiosondes, the Advanced Navy Aerosol Model (ANAM), and the Global Aerosol Dataset (GADS)” [6]. Point-based methods on the other hand would include various calculation models. Examples of some point-based methods include: NAAPS/FAROP (Navy Aerosol



Analysis and Prediction System/Forecast of Aerosol Radiative and Optical Properties) and AOD (Aerosol Optical Depth). In addition to the previously mentioned point-based models, AFIT provided a path radiance program that enables the user to define ground level conditions.

Another example that displays the current inability to sufficiently limit deviation in path radiance calculations on small timescales comes from the Space Dynamics Laboratory at Utah State University. The SDL (Space Dynamics Laboratory) is currently researching a technique to aid in SensorCAD modeling. The SensorCAD models that have been developed provide a very thorough depiction of a signal analysis situation involving air and spaced based sensors. The models take into account natural phenomena such as, “solar system celestial objects, stars, zodiacal light” [8], as well as surface optical properties and attitude control of the sensor’s vehicle. In order to improve upon the vast number of capabilities that the SensorCAD models present, a research project has been initiated between SDL and AFIT. The research consisted of enabling the user to define ground level atmospheric quantities that could be used to describe higher altitude conditions.

### **Problem Statement**

In summary, there are two problems which have been noticed with respect to current atmospheric radiative transfer programs:

1. Most radiative transfer models do not easily allow detailed weather input including probabilistic meteorological data and aerosol information. The program used to model the atmosphere for this project (LEEDR-Laser Environmental Effects Definition and Reference) does, but it needs a surface data input option.
2. Most LBL (Line-by-Line) radiative transfer models require a lot of computation time to compute transmission for path radiance calculations, over “bands” of the spectrum.

Band models are able to accurately calculate transmission faster over narrow and wide bands of the spectrum, while losing some accuracy at individual lines.

In reference to the first point made, turbulence in the atmosphere induces changes in the conditions of the atmosphere up until a certain altitude. This well-mixed region of the lower atmosphere is typically called the boundary layer. The reason for this is due in part to the transfer of energy from the ground to the upper atmosphere. This process can be described in general, by analyzing the amount of solar radiation and wind in the boundary layer. Initially, energy is transferred to the ground by solar radiation. Depending on the time of day and season, a certain amount of energy is radiated from the ground. The amount of energy in turn induces motion in the molecules above the ground. As a result of the induced motion as well as wind (resulting from pressure differences in the atmosphere), a mixing of molecules occurs, which in turn transfers energy to higher altitudes. The amount of energy being transferred, as one would suspect, ultimately affects the concentration of the molecules. For path radiance calculations, in which a certain path (vertical or horizontal) is considered, transmission is ultimately affected by the number of molecules (as well as aerosols) that the radiation comes into contact with. In summary, in order to accurately portray the transmission in a certain atmosphere, knowledge of the surface conditions is required.

In addition to accurately modeling the atmosphere, the amount of time to calculate the transmission is important. Current radiative transfer models that use a LBL algorithm, calculate the transmission at several points along the user's path. At each point, the concentration of the molecules (and aerosols) as well as the radiation at every angle with respect to that point, is factored in to the transmission calculations. In order to

speed up the calculations, a Band Model referred to as the Correlated-k, will be implemented. The Correlated-k distribution, in summary, analyzes the distribution of the measured effects of the molecules and aerosols on the radiation. In its final form, it allows the user to calculate the transmission, by strictly analyzing the conditions at the end of the user's path.

### **Approach**

In order to address the problems previously discussed, an in-house atmospheric radiative transfer program called LEEDR was chosen to be modified. Briefly, the program allows the user to define the atmosphere in terms of location, rain/cloud events, path length, as well as some other more advanced options, and perform LBL transmission calculations.

Currently, LEEDR has the capability for the user to incorporate a variety of previously defined atmospheres, which contain information pertaining to specific atmosphere variables, such as pressure, site altitude, temperature, and lapse rates. The user has a choice between an ocean atmosphere, standard atmosphere (locations over land), ExPERT (Extreme and Percentile Environment Reference Tables) atmospheres at specific land locations, and a user-defined Microsoft Excel format atmosphere. In order to obtain the ground level temperature, pressure, etc. for the user-defined location, each atmosphere relies on averages of atmospheric data such as temperature, pressure, humidity, and wind speed over a certain time period or season. Taking the ExPERT atmosphere for example, the selection of this atmosphere incorporates averaged variables such as: the altimeter, dewpoint, relative humidity, absolute humidity, specific humidity, temperature, wind speed, cloud coverage, weather occurrence, yearly min/max, and

diurnal temperature change. Most of these values are based on seasonal and time-of-day averages for the chosen site. The user-defined Microsoft Excel atmosphere on the other hand, allows the user to upload an excel file containing two sheets of inputs. The first sheet contains the following: path altitude information, atmosphere type, aerosol concentration type, molecular concentration model, turbulence model, and wind model type. While the first sheet describes scenario geometry and specific algorithms used, the second sheet delves more into the individual atmospheric quantities such as temperature, dewpoint, pressure, relative humidity, molecular absorption, and turbulence.

In response to the previously defined atmospheric profiles, the creation of a user-defined atmospheric variable tab has been proposed. The tab would essentially allow the user to override some of the ground level variables that the program imports from the atmospheric databases. Once the user has specified the ground level value, lapse rates previously incorporated in the program will allow the variables to be extrapolated to higher altitudes. In order to account for variables that the user might not be able to measure or calculate, the tab will work in unison with the ExPERT atmosphere. The ExPERT atmosphere as stated before, contains atmospheric data corresponding to particular sites around the world. Thus, the addition of this tab will allow the program to more accurately characterize a specific site at a specific time.

In addition to incorporating a user-defined ground level tab, modification of LEEDR's current transmission calculation algorithm is a part of this project. The current LEEDR program utilizes a line-by-line calculation technique. In order to calculate the transmission at the end of the user's path length, the program first calculates the extinction at numerous points along the path. As one might guess, this process is rather

time consuming. At each section of the user's path length, the program has to determine the concentration of aerosols, molecules, as well as the transmission effects from cloud/rain events. In order to improve upon this attribute of the program, a new method will be implemented into LEEDR.

### **Document Outline**

This research paper is divided into five cohesive sections. The first segment is the present section, the introduction. The subsequent section is entitled Literature Review. In this section, discussion will be primarily concerned with the LEEDR program and the history leading up to, and including, the transmission algorithm that will be incorporated into this program. In terms of the LEEDR program, more information will be presented on the models and atmospheric principles used to create a radiative transfer atmosphere. As for the transmission algorithm, information pertaining to evolution of this method will be presented to the reader. The next section, entitled Methodology, will explain the additions to the LEEDR program in a more mathematical sense. Discussion of the particular transmission algorithm implemented into LEEDR will be discussed in more detail, as well as insight on how the user-defined ground level values become integrated into LEEDR's calculations. Following this section, an implication of the results of this project will be given. Lastly, a summary and suggestions of future research will be presented to the reader.

## II. Literature Review

### LEEDR (Laser Environmental Effects Definition and Reference)

LEEDR was initially developed with two goals in mind. Quoting text from a research paper by Fiorino et al., LEEDR enables the user to, "...create correlated, physically realizable vertical profiles of meteorological data and environmental effects such as gaseous and particle extinction, optical turbulence, and cloud free line of sight" [5:2]. This program also allows, "...graphical access to and export of the probabilistic data from the Extreme and Percentile Environmental Reference Tables (ExPERT)" [5:2].

There are three input tabs incorporated into the program. The first tab, entitled "Location", creates many of the features used to depict the atmosphere. The user has several options to choose from including: the particular site used for the radiative transfer calculations, the molecular effects model, the aerosol effects model, the ground visibility, and boundary layer height. In terms of the location of the site, the user can select a site in number of ways. A site can be chosen by indicating the longitude and latitude of the desired location in a text box. If the specific latitude and longitude is unknown, the user has the choice of selecting a site from a two-dimensional world map, located next to the latitude and longitude text box. The two-dimensional world map enables the user to select any location in the world by simply pointing the mouse cursor and clicking. In order to aid in this process, two additional features have been integrated into the map. First, alongside the map, above the latitude and longitude text box, there are two zoom buttons, which allow the user to focus in on a particular state, province, or country. Secondly, located on the map itself are 408 ExPERT sites, which are indicated by red and yellow circles (Figure 1).

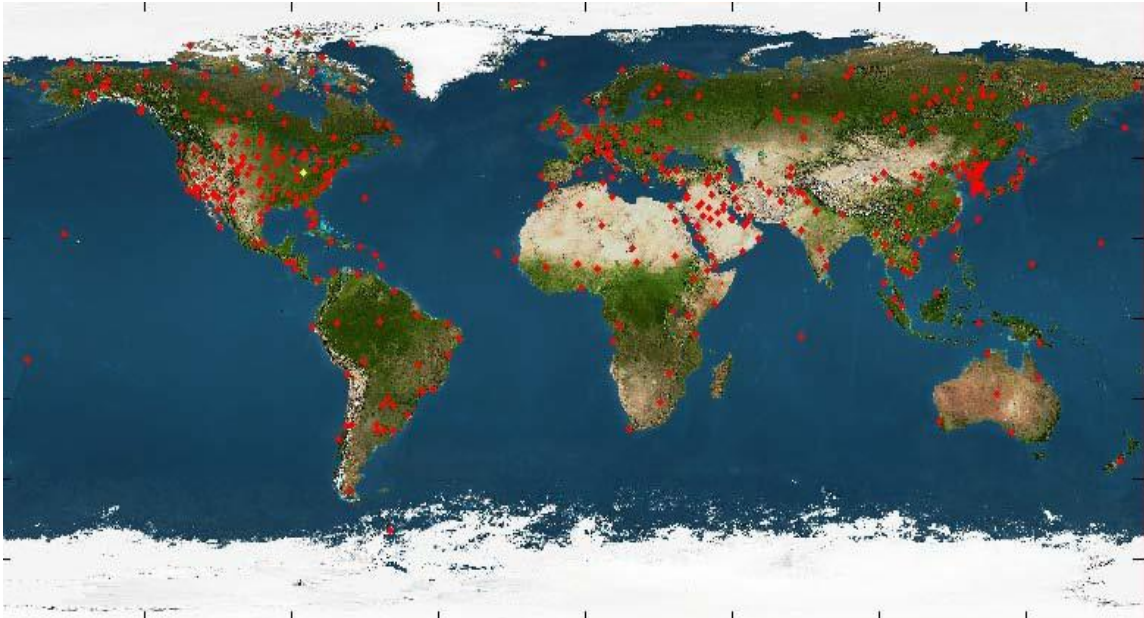


**Figure 1. The ExPERT sites in LEEDR**

The ExPERT sites (which will be discussed later in the Methodology section), contain measured data pertaining to a particular site. Thus, radiative transfer calculations and upper air measurements are more accurate for locations near these sites, than simply clicking on a location near the ExPERT site. In order to select an ExPERT site, the user must click on the “Use this Site” button, located below a separate set of text boxes on the Location tab, displaying the nearest ExPERT site, as well as the latitude and longitude points of that site. The user however, does not have to select an ExPERT site. Any location over land or water will suffice in creating a user-defined atmosphere.

The molecular effects model, which will be discussed in more detail in the next section entitled “LEEDR (Absorption/Scattering)”, provides the user with three options. The first option entitled “Calculations”, utilizes Rayleigh Scattering and the HITRAN

2004 database for molecular absorption, to compute the desired reduction or intensification of the transmission. The second option, entitled “Load from Excel”, as the name would suggest, allows for the integration of an excel file into LEEDR, which specifies the molecular absorption and molecular scattering in  $\text{km}^{-1}$ . Lastly, the user can also specify coefficients of the absorption and scattering in connection with scattering and absorption equations (Absorption =  $Ae^{-\text{altitude}/B}$ , where A is in  $\text{km}^{-1}$  and B is in km, and Scattering =  $e^{A+(B*\text{altitude})}$ , where A is unit less and B is in  $\text{km}^{-1}$ ).

The aerosol effects model is constructed in a similar manner, in that the user can select a previously defined model, or they can define a set of coefficients depicting absorption and scattering phenomena. In the dropdown menu under “Aerosol Effects Model”, the user once again has three different options. The first option allows the user to once again define coefficients describing the absorption and scattering effects on radiation (Absorption = Scattering =  $Ae^{-\text{altitude}/B}$ , where A is in  $\text{km}^{-1}$  and B is in km). The second option, somewhat similar to the “Molecular Effects model”, uses the GADS aerosol model. This model, in more detail, incorporates the effects of Wiscombe Mie model into the calculations pertaining to transmission. In summary, the size of the particle in relation to the wavelength of the radiation is the primary focus for how transmission is going to be affected. The third and final option presents the user with the choice of selecting from a variety of predefined aerosol distribution models. As mentioned before, LEEDR has several (18 to be exact) pre-existing models to select. These options include maritime aerosol models, continental average aerosol models, arctic models, brownout models, and even some MODTRAN (Moderate Spectral Resolution Atmospheric Transmission) models.



In the next tab, entitled “Atmosphere”, the user is given the opportunity to define the turbulence model as well as the wind and clouds/rain model. There are eight different turbulence models currently in LEEDR. These models include: Hufnagel-Valley 5/7 (HV 5/7), CLEAR 1 (Critical Laser Enhancing Atmospheric Research), None (Vacuum), Climatological  $C_n^2$ , SOR (Starfire Optical Range) Special, Constant  $C_n^2$ , NSLOT (Navy Surface Layer Optical Turbulence)  $C_n^2$  and Tunick. Each turbulence model, to summarize, uses different assumptions to help model the variation in atmospheric quantities, which ultimately results in changes in the index of refraction structure constant, or  $C_n^2$ . Along with the turbulence models, there are four different wind profile methods. The four different methods consist of: the Climatological Wind Profile, Bufton Wind Profile, Excel File Wind Profile, and the Ocean Wind Profile. Lastly, LEEDR incorporates several cloud and rain scenarios. The user has numerous options including two different types (that being maritime and continental) of cumulus clouds, and stratus clouds. In addition, the user can specify a fog deck, drizzle (2mm/hr), very light rain (5mm/hr), light rain (12.5mm/hr), moderate rain (25mm/hr), heavy rain (50mm/hr), and extreme rain (75mm/hr). In order to more accurately account for these effects in the atmosphere, LEEDR enables the user to define the region in which they are occurring. Alongside dropdown menu consisting of the rain and cloud events, the user has the opportunity to select an upper and/or lower altitude for the chosen event.

The last tab, which is referred to as the “Laser/Geometry” in the LEEDR program, gives the user the opportunity to select their path length, as well as the wavelength of the radiation being observed. In terms of the path length, the user the option of selecting a purely azimuthal or zenith, beginning and ending location. As for

the wavelength of radiation, there are currently 20 different wavelengths (ranging from 0.355  $\mu\text{m}$  to 10.6  $\mu\text{m}$ ) incorporated into LEEDR, as well as a user-defined wavelength option enabling the user to select any wavelength from 0.4  $\mu\text{m}$  to 8.6  $\mu\text{m}$ .

### **LEEDR (Absorption/Scattering)**

When specifying a molecular or aerosol effects model, there are numerous models which the LEEDR program uses to perform these calculations. In terms of the molecular effects model, as previously stated, there are three different options that the user has the choice of selecting. One can obtain a molecular effects model through calculations, one can load their own molecular model, or one can create their own model by specifying absorption and scattering coefficients. The aerosol effects model, as was the case with the molecular effects model, has three different options. The first option allows the user to select the GADS aerosol model. The second and third options allow the user to select from other regionally pre-defined models or create their own model, respectively.

Focusing on previously research models, and excluding the equation and excel based methods, the aerosol concentration in particular, is modeled by both the GADS and ANAM [5:2-4]. The GADS aerosol model creates the aerosol distribution by utilizing previous data collection measurements to model 12 different aerosol types, along with their relative abundances in different regions, and under different circumstances. Some of the aerosol types, according to d'Almeida et al, consist of: arctic, antarctic, clean-continental, average-continental, urban, desert, clean-maritime, maritime-mineral, maritime-polluted [4:147-168]. Each of the different aerosol types is made to be defined by a certain cross section, single scatter albedo, and asymmetry factor. D'Almeida also notes that, phenomena which induce changes in the concentration of the aerosols include

factors such as seasonal-migration of the climatic belts (e.g. polar fronts, intertropical convergence zones, etc.), and abundance of water vapor. In the LEEDR program, GADS model data is averaged on a 5° by 5° area. In order to model aerosol distribution over a body of water however, the program reverts to the ANAM model. Concentration values for this model unlike the GADS model, are based off measurements pertaining to areas 1° by 1°, from “...just above the sea surface up to a few meters (~10 m)” (above 10 m, relations between concentration and wind speed can be used) [7:42]. It is noted in the paper entitled *Characterizing large aerosols in the lowest level of the marine atmosphere*, that aerosol distribution with height is based off of the Rotorod technique, which describes the presence of large aerosols (> 10 μm) [7:44] near the water’s surface. In summary, the Rotorod technique employs a device which consists of two stainless steel rods coated in Silicone, connected to a platform made to rotate in an azimuthal direction. When initiated for testing, the motor causes the platform to rotate, which in turn forces the stainless steel rods, which were initially at rest on the platform, to rise up. Testing of aerosol distribution and size can then be performed by observing the steel rods with a microscope. The results of tests (i.e. distribution of aerosols pertaining to a particular radius) utilizing the Rotorod technique were then modeled by a lognormal function.

Molecular and aerosol scattering are determined from Rayleigh theory and the Wiscombe Mie model, respectively. To summarize, both forms of scattering present in LEEDR are based off of a size parameter. In equation form, the size parameter is represented as:

$$x \equiv \frac{2\pi r}{\lambda} \quad (1)$$

where  $r$  is the *radius* of the particle, and  $\lambda$  is the *wavelength* of the radiation. One encounters Rayleigh Scattering when the size parameter is between  $x=0.2$  and  $x=0.002$ . From an observational standpoint, Rayleigh Scattering is present for raindrops and drizzle, when viewed in the microwave. Mie Scattering, on the other hand, encompasses a much wider range. The size parameter associated with Mie Scattering includes  $x=2000$  and  $x=0.2$ . A situation that would involve Mie Scattering would include cloud droplets (radius  $\sim 10\mu\text{m}$ ) in the thermal infrared ( $4\mu\text{m}$  to  $50\mu\text{m}$ ). In general, Rayleigh Scattering involves situations where the particle is, "... sufficiently small relative to the wavelength – i.e.,  $|m|x \ll 1$  – every part of the particle simultaneously experiences the same externally imposed oscillating electric field" [11:347]. This in turn causes the particle to become polarized. The resulting dipole creates an electric field, which interacts with the incident electric field. Ultimately, one arrives at an equation depicting the observed intensity, which is:

$$I \propto \omega^4 (1 - \sin^2 \Theta \cos^2 \Phi) \quad (2)$$

where  $I$  is the *intensity* ( $\text{W m}^{-2} \text{sr}^{-1}$ ),  $\omega$  is the *frequency* of the incident radiation,  $\Phi$  is the *polar angle* of the incident wave, and  $\Theta$  is the *angle with respect to the incident wave and observed point*. From this equation, conclusions can be made concerning the scattering and extinction efficiencies. If one considers the size parameter to consist of a power series, one can in turn derive the extinction and scattering coefficients. Important relations that can be drawn from this assumption are represented in the following two equations:

$$Q_s \ll Q_a \approx Q_e \quad (3)$$

where  $Q_s$ ,  $Q_a$ , and  $Q_e$  are the *scattering, attenuation, and extinction coefficients*, respectively.

$$\tilde{\omega} \equiv \frac{Q_s}{Q_e} \propto x^3 \quad (4)$$

where  $\tilde{\omega}$  is the *single scatter albedo* (represents ratio of scattering and extinction). With these two relations, one can take the analysis further and in turn gain an understanding of how the scattering and extinction effects the transmission of the radiation. Focusing on the last equation (4), one can conclude that scattering can be ignored, due to the size parameter region that Rayleigh Scattering encompasses. After taking this into account, and adding the basic definition of mass absorption coefficient, one ultimately arrives at:

$$\beta_a = k_a \rho \quad (5)$$

where  $\beta_a$  is the *volume absorption coefficient* ( $\text{km}^{-1}$ ),  $k_a$  is the *mass absorption coefficient* ( $\text{m}^2/\text{km}$ ), and  $\rho$  is the *density of the absorbing material* ( $\text{kg}/\text{m}^3$ ). This result can be summed up, using an example consisting of clouds and water vapor, by, “...for radiation passing through a cloud of sufficiently small absorbing particles, the total absorption is equal to  $k_a$  times the total mass path, regardless of the exact sizes of the constituent particles” [11:357]. Mie Scattering, on the other hand, uses the Maxwell’s equations, along with the assumption of a homogeneous sphere, to create extinction and scattering coefficients. The extinction coefficient in this case, is:

$$Q_e = \frac{2}{x^2} \sum_{n=1}^{\infty} (2n+1) \Re(a_n + b_n) \quad (6)$$

where  $x$  is the *size parameter*,  $m$  is the *relative index of refraction*,  $\Re$  is the real component, and  $a_n$  and  $b_n$  are “*Mie scattering coefficients and are functions of  $x$  and  $m$* ” [11:359]. The scattering coefficient in turn, is:

$$Q_s = \frac{2}{x^2} \sum_{n=1}^{\infty} (2n+1)(|a_n|^2 + |b_n|^2) \quad (7)$$

Once again, analyzing this result in terms of the transmission of the radiation, some interesting conclusions can be drawn. Depending on the size parameter, one can see differing amounts of forward and backward scattering. As the size parameter is increased from  $x=0.1$  to  $x=10,000$ , one observes mainly forward scattering, initially. However, as  $x$  begins to approach 10,000, the percentage of forward scattering and backward scattering becomes equal. This feature is different from Rayleigh Scattering, in which forward and backward scattering was primarily equal for all small values of  $x$ .

### **LEEDR (Turbulence Models)**

In the LEEDR program, under the “Atmosphere” tab, there are eight different turbulence models that the user has the option of choosing. These models include: HV 5/7, CLEAR 1, None (Vacuum), Climatological  $C_n^2$  (applicable to ExPERT, mid-latitude and desert sites only), SOR Special, Constant  $C_n^2$ , NSLOT  $C_n^2$  (for ocean sites only), and Tunick. Each of the models calculates, under different circumstances (isoplanctic angles, etc.), the value of refractive index structure constant  $C_n^2$ . The refractive index structure constant essentially measures the efficiency of radiation propagation, as a result of changes in the distribution of material in the atmosphere. From this quantity, one can in turn account for changes in transmission.

The refractive index structure constant measures the amount of deviation in the refractive index. Changes in the refractive index are seen to be the most prominent due to disparities in temperature and relative humidity. Temperature and humidity variations arise when one begins to view the atmosphere as it truly is, a fluid. From this vantage point, it becomes evident that the reason for the variation in our refractive index structure constant is in due part to convection within the atmosphere. The resulting affects of convection, which are induced by differing areas of pressure associated with weather systems, in turn cause differences in temperature, and water vapor.

In areas of differing indices of refraction, one would obviously notice problems arising in any imaging application. In terms of laser beam propagation, the effects that can be observed due to optical turbulence include, “beam wander and broadening” [2:159]. For remote sensing applications, optical turbulence can cause “image dancing and blurring” [2:159].

In order to describe the variation of the atmospheric constituents, initial consideration was given to the Navier-Stokes equation. The Navier-Stokes equation depicts the turbulence that arises in a fluid due to different velocity regions, as well as particle collisions. However, due to the problem of closure, new methods had to be developed to explain deviations in the atmosphere. One of the first methods developed from the observed limitation of the Navier-Stokes equation in the atmosphere, was the Kolmogorov model. According to Kolmogorov, the atmosphere is made up of different sized eddies. The eddies that are present in the atmosphere, Kolmogorov reasoned, were due to “convection and wind shear” [2:167] (Figure 2). According to the model, big eddies exist higher in the atmosphere, and successively smaller eddies are observed as

one gets closer to the ground. Inside each eddy, Kolmogorov assumed that the atmosphere was homogeneous, isotropic, and ergodic. That is to say, there are an equal number of large and small molecules and aerosols distributed uniformly in each direction away from a certain point, and that each state that they could be in is equally likely. A famous quote by Lewis Fry Richardson describes the interactions that take place between eddies, “Big whirls have little whirls, that feed on their velocity; and little whirls have lesser whirls, and so on to viscosity”. After going through quite a bit of math concerning the velocity distributions that reside in each level of the atmosphere, and the structure function (represents the mean square difference in the index of refraction at points separated by a distance  $r$ ), one ultimately arrives at a piecewise function depicting the index of refraction:

$$D_n(r) = \begin{cases} C_n^2 r^{2/3} & l_0 < r < L_0 \\ C_n^2 l_0^{-4/3} r^{2/3} & r < l_0 \end{cases} \quad (8)$$

Based on this equation, one can see that Kolmogorov’s Theory attempts to model the deviation in turbulence through the structure constant  $C_n^2$ , which he deduces, varies in both time and space. Figure 2 illustrates this concept:



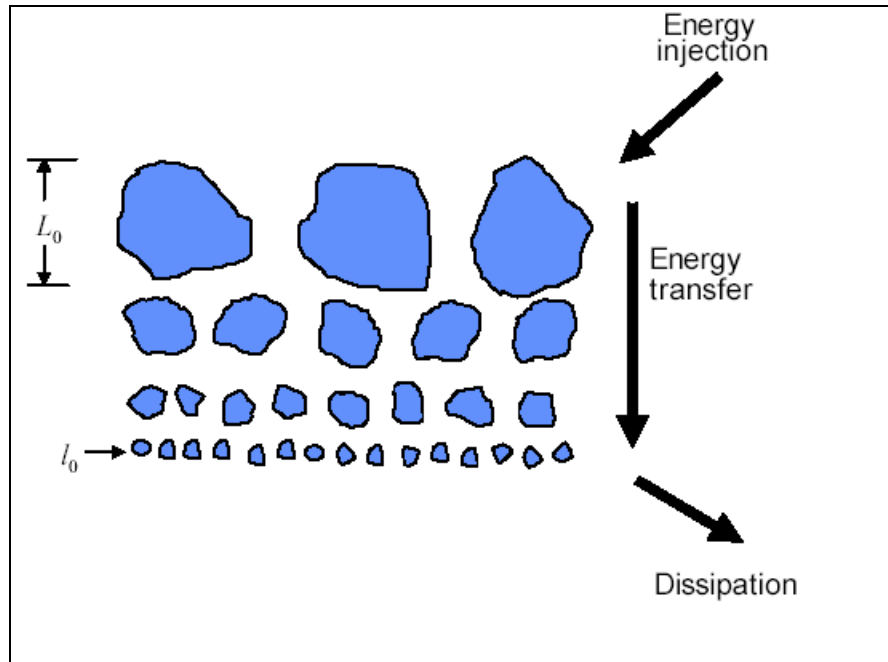


**Figure 2. Kolmogorov's Model of Variation in the Atmosphere**

where  $L_0$  and  $l_0$  refer to diameters of *homogeneous, ergodic, and isotropic areas*. The resulting values of the refractive index structure constant for Kolmogorov's model show that, atmospheres with structure constants around  $C_n^2 \sim 10^{-17} \text{ m}^{-2/3}$  experience 'weak' turbulence, while atmosphere's with  $C_n^2$  values  $\sim 10^{-13} \text{ m}^{-2/3}$  experience a stronger form of turbulence.

Since the development of Kolmogorov's turbulence model, there have been two proposed models that are used in practice. These models are discussed in more detail in the journal article entitled, *Propagation through Atmospheric Optical Turbulence* by R. R. Beland [2]. The first sets of models are labeled as the Model Optical Turbulence Profiles. These models were created from experimental observed data. According to the text, these models differ from the previous Kolmogorov model in that, they, "were derived by curve-fitting a piecewise-continuous polynomial to a variety of measurements

(e.g. scintillometer data, acoustic sounder, aircraft, and others)” [2:218]. The turbulence model from LEEDR which is categorized under the Model Optical Turbulence Profiles, is the CLEAR 1 model. The other category of models which were proposed, are the Parametric Models. In the text, these models are described as having, “...parameters in an attempt to incorporate some dependencies on winds and meteorology and to model the complexity of actual  $C_n^2$  measurements” [2:221]. The HV 5/7 model is one of the most recognized models from this category. Parameters that are utilized in the HV 5/7 include the strength of the surface turbulence, speed of high altitude winds, the atmospheric coherence length, and isoplanatic angle.

### **LBL (Line-By-Line Calculations)**

As noted in the text *A First Course in Atmospheric Radiation* by Grant W. Petty [11], there are a variety of ways that one could use to analyze transmission and extinction in the atmosphere. The first method that Petty introduces to the reader is the LBL technique. As was mentioned previously, LEEDR includes a line-by-line transmission calculation algorithm for wavelengths ranging from ultraviolet to radio frequencies.

The LBL technique is often considered to be a tedious but extremely accurate method for computing transmission calculations. The reason for this is due in part to the number of computations that have to be performed throughout the atmosphere, as well as the amount of information being filtered into the absorption calculations. Due to the complexity that arises when attempting to model transmission in the active atmosphere however, a few assumptions have been made for the LBL approach. One assumption is that when computing transmission values, a plane-parallel (in which atmospheric quantities are assumed to vary more substantially in the vertical direction, than the

horizontal) atmosphere is to be utilized. Another assumption presents itself when one considers the broadening of the absorption lines that occur due to pressure and Doppler broadening. In the case of pressure broadening, collisions with other molecules induce absorption lines resembling a broadened Lorentz line shape. Doppler line shapes on other hand consist of lines that have a more narrow shape, and a half width that is dependent on temperature. The question that arises though is where one should cut off the line shape. One approach that has been used is to multiply the line by certain values ranging from 0 to 1. To clarify, one would multiply the peak by 1, and the rest of the line by a specific value that would decrease to 0, when a sufficient amount of absorption has been considered.

In the discussion of the LBL technique, it is often helpful to begin with the basic definitions concerning the transmission of radiation. In most introductory atmospheric science or spectroscopy classes, one of the first laws pertaining to radiation transmission that one comes across is Beer's law. Beer's law states that, "...the intensity of a beam of monochromatic radiation falls off exponentially as it traverses a uniform medium" [11:78]. The reason for the reduction in intensity is due in part to the presence of aerosols and molecules, which alter the radiation. This leads us to the basic definition of transmittance for monochromatic radiation, which states:

$$t(x) \equiv \frac{I(x)}{I_0} = e^{-\beta_a x} \quad (9)$$

where  $I(x)$  is the *received intensity* ( $\text{Wm}^{-2}\text{sr}^{-1}$ ),  $I_0$  is the *initial intensity* ( $\text{Wm}^{-2}\text{sr}^{-1}$ ),  $\beta_a$  is the *absorption coefficient* ( $\text{km}^{-1}$ ), and  $x$  is the *distance* (km) that the radiation has traveled.

Taking the analysis for transmission a step further, one can begin to apply it to a plane-parallel atmosphere. For the LBL calculations, the optical depth, which represents the amount of extinction (absorption and scattering) that will occur to the radiation along its path, is defined as:

$$\tau_{\bar{\nu}}(z_1, z_2) = \left| \int_{z_1}^{z_2} \beta_{a_{\bar{\nu}}}(z) dz \right| \quad (10)$$

where  $\tau_{\bar{\nu}}$  is the *optical depth*, which is dependent upon wavenumber, and  $\beta_{a_{\bar{\nu}}}(z)$  is the *volume absorption coefficient* ( $\text{km}^{-1}$ ). In order to aid in the comprehension of the previous equation, one can in turn break down the volume absorption coefficient into quantities consisting of the density of the absorbers and scatters, as well as the mass absorption coefficient. The mass absorption coefficient accounts for the mass of the absorbing and scattering material. A famous experiment consisting of Petri dishes filled with milk, water, and India ink [17] illustrates this coefficient. The results found that based on the amount of India ink and milk applied to the Petri dish, the transmission would be affected. The resulting volume absorption coefficient is:

$$\beta_{a_{\bar{\nu}}}(z) = \sum_{i=1}^N \rho_i(z) k_{a,i}(z) \quad (11)$$

where  $\rho$  is the *local density* ( $\text{kg}/\text{m}^3$ ) at a *height*  $z$  (m), and  $k$  is the *mass absorption coefficient* ( $\text{m}^2/\text{kg}$ ) for the particular  $i$ th constituent.

Thus, for a typical absorption spectrum which consists of many peaks and valleys along the wavelength or wavenumber spectrum, the LBL method calculates transmission at each level of the atmosphere by utilizing the following equation:

$$T_{\tilde{\nu}}(u) = \exp\left(-\int_{z_1}^{z_2} \rho(z)k_{\tilde{\nu}}(z)dz\right) \quad (12)$$

where  $k_{\tilde{\nu}}$  is the *mass extinction coefficient* ( $\text{m}^2/\text{kg}$ ) and  $\rho(z)$  is the *density* ( $\text{kg}/\text{m}^3$ ) of the absorbing gas.

### **Band Models (Wide and Narrow Band Models)**

In order to improve upon the calculation time required for LBL calculations, band models were created. In terms of LEEDR, calculation times over a user-defined part of the interval with LBL calculations could range on the order of minutes to hours, depending of the level of accuracy given to the atmospheric profile. In order to speed up the calculation time, band models assume certain characteristics of the lines in the spectrum.

Beginning the discussion with the definition of absorptance (i.e. how much radiation of a particular wavenumber is absorbed), which is defined as:

$$A_{\tilde{\nu}}(u) = 1 - T_{\tilde{\nu}} = \frac{1}{\Delta\nu} \int_{\Delta\nu} (1 - e^{-k_{\tilde{\nu}}u}) d\nu \quad (13)$$

where  $A$  is the *absorptance*,  $T$  is the *Transmission*,  $\Delta\nu$  is the *wavenumber domain* ( $\text{m}^{-1}$ ),  $k_{\tilde{\nu}}$  *absorption coefficient* ( $\text{m}^2/\text{kg}$ ), and  $u$  is the *path length* ( $\text{kg}/\text{m}^2$ ). In order to aid in analyzing how the absorptance varies with changing path length and absorption, the equivalent width was defined. Mathematically, the equivalent width is defined as:

$$W \equiv \int_{\Delta\tilde{\nu}} 1 - e^{-\tau_{\tilde{\nu}}} d\tilde{\nu} \quad (14)$$

The equivalent width represents a square line in the absorption spectrum that absorbs the same amount of radiation as the observed absorption data. In the weak line limit, in which the optical depth is  $\tau_{\tilde{\nu}} \ll 1$ , the equivalent width can be written as:

$$W = Su \tag{15}$$

where  $S$  is the *line strength* ( $\text{cm}^{-1}/\text{molecule cm}^{-1}$ ) and  $u$  is the *path length* (m). What this ultimately tells us is that, “total path absorption is proportional to the line strength and the mass path  $u$ , *irrespective of line shape*” [11:289]. In terms of a strong line limit (where the opposite is true  $\tau_{\tilde{\nu}} \gg 1$ ), the equivalent width becomes,

$$W = 2\sqrt{S\alpha u} \tag{16}$$

where  $S$  is the *line strength*,  $u$  is the *mass path*, and  $\alpha$  is the *line half-width*.

Two generally agreed upon band transmission models utilize the previously discussed assumption of equivalent width. The first model that will be mentioned is the wide-band transmission model. These models are typically used when accuracy is of the highest importance. The other type of band model, that being narrow-band transmission models, focus more on computation speed rather than accuracy. In order to achieve a faster transmission result, narrow-band models divide the desired part of the spectrum into parts based on certain characteristics, including: the number of lines, their position and strength, and Planck’s Function. The band-averaged transmission can in turn be found by making assumptions concerning the orientation of the observed absorption lines. A few models typically used in practice include the Elasser Band Model, and the Malkmus Band Model.

In the case of the Elasser Model, a periodic Lorentzian distribution is assumed for the absorption lines. For this model, a set of absorption lines can be modeled by using hyperbolic sines and cosines.

$$k_{\tilde{\nu}} = \frac{S}{\delta} \frac{\sinh(\beta)}{\cosh(\beta) - \cos(\gamma)} \quad (17)$$

where  $k_{\tilde{\nu}}$  is the *absorption coefficient* which is dependent upon wavenumber,  $S$  is the *line intensity*,  $\alpha$  is the *half-width*,  $\delta$  is the *line spacing*, and  $\beta$  and  $\gamma$  are *parameters which depend upon the line spacing, wavenumber, and half-width*. In equation form,  $\beta$  and  $\gamma$  are represented in the following manner.

$$\begin{aligned} \beta &= \frac{2\pi\alpha}{\delta} \\ \gamma &= \frac{2\pi\tilde{\nu}}{\delta} \end{aligned} \quad (18)$$

In order to account for a larger or smaller separation between absorption lines, one often utilizes a “grayness parameter”, which is defined as:

$$y \equiv \frac{\alpha_L}{\delta} \quad (19)$$

where  $\alpha_L$  is the *Lorentzian half-width*. One can begin to see the functionality of the equation depicting the absorption coefficient (i.e. equation 17), when one varies the grayness parameter. In reference to equation 19, if one makes  $y$  large, the resulting set of the absorption lines will have small line spacing parameter  $\delta$ , and thus will tend to overlap. If  $y$  is small, the opposite will be true. A small  $y$  would entail large line spacing, and thus a lot of space in-between absorption lines. After inserting the grayness parameter into equation 17, the absorption coefficient becomes:

$$k_{\tilde{\nu}} = \frac{S}{\delta} \frac{\sinh(2\pi y)}{\cosh(2\pi y) - \cos\left(\frac{2\pi\tilde{\nu}}{\delta}\right)} \quad (20)$$

Inserting the previous equation (equation 20) into the equation of spectral transmittance (equation 21), one arrives at the following two equations for transmittance with the Elasser Band Model (equation 22).

$$T_{\tilde{\nu}}(u) = \int_{\Delta\tilde{\nu}} e^{-\tau} \frac{d\tilde{\nu}}{\Delta\tilde{\nu}} = \int_{\Delta\tilde{\nu}} \exp\left(-\int_u \sum_j k_{\tilde{\nu},j}(u) du\right) \frac{d\tilde{\nu}}{\Delta\tilde{\nu}} \quad (21)$$

where  $u$  is the *mass path length*.

$$T_{\tilde{\nu}}(u) \approx \begin{cases} 1 - \text{erf}\left(\pi y \sqrt{2u}\right) & u \gg 1 \\ \exp(-Su / \delta) & \text{Large } y \text{ (order 10 or greater)} \end{cases} \quad (22)$$

where  $\text{erf}$  is the *error function*.

The Malkmus model, on the other hand, does not assume a periodic motion (which is only observed with linear molecules such as  $\text{CO}_2$ ). Instead absorption lines are assumed to occur at random positions throughout the domain. In addition, line strengths are described according to an exponential model, which states:

$$p(S) = (1/\bar{S}) \exp(-S/\bar{S}) \quad (23)$$

where  $S$  is the *line strength*, and  $\bar{S}$  is the *mean line strength* from 0 to  $\infty$ . Under the same conditions as the Elasser Model, transmission is defined as:

$$T_{\tilde{\nu}}(u) \approx \begin{cases} \exp\left[-\frac{\pi\alpha_L}{2\delta} \left\{\sqrt{1 + \frac{4\bar{S}u}{\pi\alpha_L}} - 1\right\}\right] \\ \exp\left[-\frac{\pi y}{2} \left\{\sqrt{1 + 8u} - 1\right\}\right] \end{cases} \quad (24)$$

### **K-Distribution/Correlated-k**



Even though the band models are able to calculate the transmission in a faster manner, certain aspects of the models can lead to deficiencies in calculation accuracy. Elasser Band Models are able to calculate transmission for, “P- and R-branches of a vibration/rotation band” [11:294]. However, accuracy is limited to linear molecules like (e.g. CO<sub>2</sub>). The Random or Malkmus Model accounts for the spectrum of “nonlinear molecules like water vapor, ozone, methane, etc.” [11:297] however, when one extrapolates this model to nonhomogeneous atmospheres, errors become apparent (e.g. Curtis-Godson approximation in the 9.6 μm band for O<sub>3</sub> [9:147]).

Recent research however, with respect to k-Distribution models, has shown much more promise in terms of calculating transmission in homogeneous atmospheres (where pressure and temperature are essentially constant). As noted by Petty, the K-Distribution model “...is a relatively recent innovation and is rapidly gaining favor in view of its ability to achieve fairly accurate results with two or three orders of magnitude less computer time than LBL methods” [11:285].

Unlike the LBL and Band Models previously mentioned, the k-Distribution method proposes a calculation method dependent upon the distribution of the extinction in the spectrum. Thus, the spectral transmission equation can be transformed from one that depends on wavenumber, to one that depends upon integration over an interval of absorption values:

$$T_{\tilde{\nu}}(u) = \int_{\Delta\tilde{\nu}} e^{-k_{\tilde{\nu}}u} \frac{d\tilde{\nu}}{\Delta\tilde{\nu}} = \int_0^{\infty} e^{-ku} f(k)dk \quad (25)$$

where  $k$  is the *volume extinction coefficient* (km<sup>-1</sup>),  $u$  is the *path length* (km),  $\Delta\nu$  is the *wavenumber interval* (cm<sup>-1</sup>), and  $f(k)$  is the *probability distribution function* (defined as

$\int_0^{\infty} f(k)dk = 1$ , where  $k_{\min}$  has been set to 0, and  $k_{\max}$  has been set to  $\infty$ ). However, even

after transforming the transmission integral from the wavenumber domain to absorption coefficient domain, transmission calculations can be extensive. Since the probability density function is mostly likely not monotonic throughout the range of absorption coefficients, a large amount of computation points could be needed to effectively compute transmission (since the integral in equation 25 can be turned into a Riemann sum). In order to reduce computation time, the cumulative probability function (commonly represented as  $g(k)$  for the k-Distribution) as a function of absorption coefficient value, can be utilized. The cumulative probability function can be obtained by integrating the probability distribution function over the desired absorption interval, starting from 0. Ultimately, what is being obtained through the cumulative probability function is the fraction of absorption values (0 through some  $k$ ), throughout the previously defined wavenumber interval. Thus, the transmission equation that was represented by equation 25 becomes equation 26, after using the cumulative probability function.

$$T_{\tilde{\nu}}(u) = \int_{\Delta\tilde{\nu}} e^{-k_{\tilde{\nu}}u} \frac{d\tilde{\nu}}{\Delta\tilde{\nu}} = \int_0^1 e^{-k(g)u} dg \cong \sum_{j=1}^M e^{-k(g_j)u} \Delta g_j \quad (26)$$

where  $T$  is the *transmittance*,  $k(g)$  is the *inverse of the cumulative probability or equivalent k function*,  $u$  is the *mass path*.

The extrapolated version of the k-Distribution method is referred to as the Correlated-k method. Essentially, whereas the k-Distribution method is accurate within a homogeneous atmosphere, the Correlated-k can be applied to path lengths in which

pressure and temperature can vary. The reason for this is due in part to overlapping absorption lines that occur due to different concentrations of molecular species in the higher altitudes of the atmosphere (a particular example includes H<sub>2</sub>O and CO<sub>2</sub> at 15μm). The proposed solution or Correlated-k algorithm proposed solution is in turn given by Liou. For an example, in which two atmospheric gases are considered, one can use the respective molecular mixing ratios (or concentrations), to compute a new exponential term in the transmittance equation. Using the transmittance equation previously defined (23), and assuming the gas lines to be statistically independent, one can in turn use the previously defined k-Distribution method to calculate the new transmission. The resulting equation is:

$$T_{\bar{\nu}}(q, q_c) \equiv \int_0^1 \int_0^1 \exp\left\{-\int [k(g_1)q_c + k(g_2)q]\rho dz\right\} dg_1 dg_2 \quad (27)$$

where  $\rho$  is the *air density* (kg/m<sup>3</sup>),  $q$  and  $q_c$  are the *mixing ratios* of the two gases, and  $k(g_1)$  and  $k(g_2)$  are the two *equivalent k functions* of the gases.

### **III. Methodology**

#### **Overview**

This chapter delves into the mathematical concerns pertaining to both sections of this research project. In terms of the User-Defined Ground Level tab, discussion of how the user's values become factored into the LEEDR program's calculations will be presented. As for the Correlated-k algorithm, the particular algorithm from which this research project's Correlated-k algorithm was model is developed, is discussed.

#### **User-Defined Ground Level Tab**

Through a newly created graphical user interface (GUI), the user is given the choice of modifying several variables that are important to the description of the atmosphere. These variables include those that are directly measurable, such as pressure and temperature, as well as other important variables, such as relative humidity, absolute humidity, dewpoint, and saturation mixing ratio.

When LEEDR is initialized, the variables on the User-Defined Ground Level tab are grayed out. It is not until the user selects an ExPERT atmosphere, that the variables are enabled for modification. Figure 3 displays the User-Defined Ground Level tab, after the user has selected an ExPERT atmosphere:

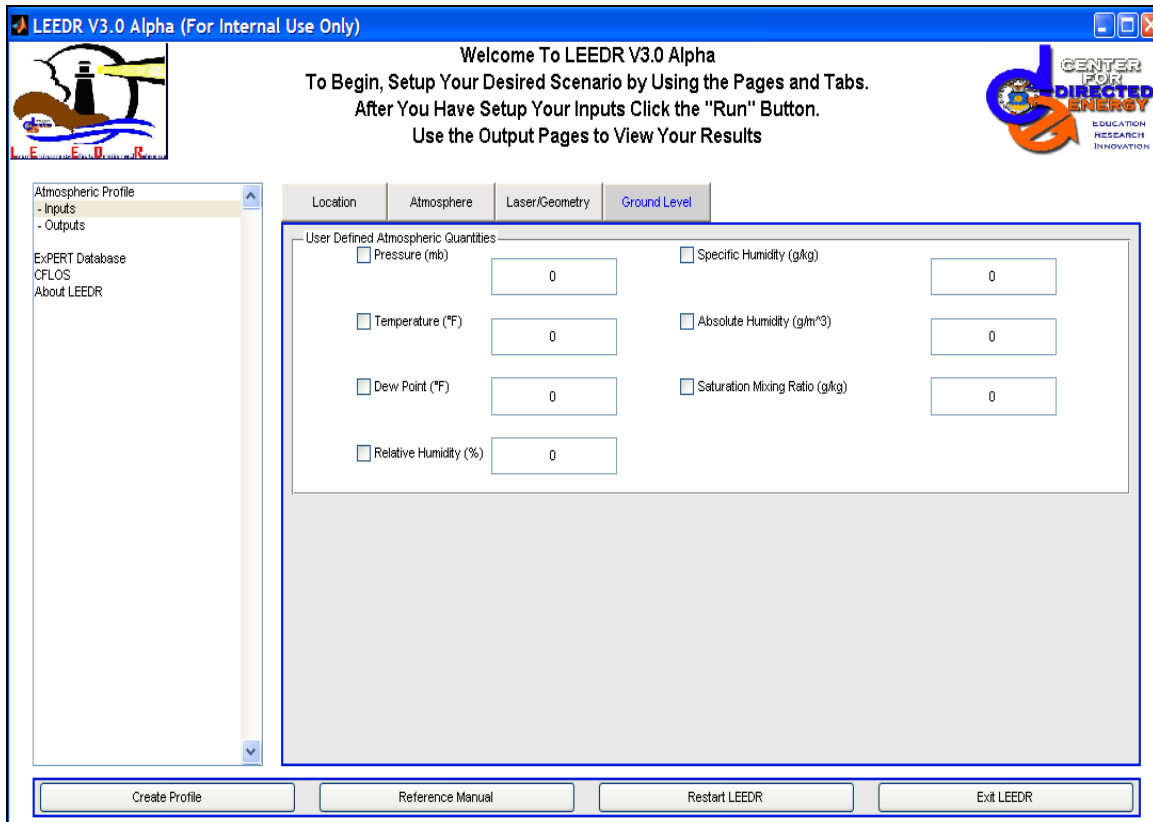


**Figure 3. User-Defined Ground Level GUI Tab Incorporated into LEEDR**

The reason for directly connecting the User-Defined Ground Level tab to the ExPERT atmosphere is that the ExPERT atmosphere already contains climatologically averaged atmospheric data pertaining to a particular site. Immediately after selecting the site, the user is given the opportunity to change the time of day (in 3-hour increments), and the relative humidity percentile (1<sup>st</sup> percentile-Dry to 99<sup>th</sup> percentile-Most Damp, in unevenly spaced increments), on the Location tab. Thus, with the addition of the ground level tab, the user has more control of the atmosphere for these sites (from the ground to the boundary layer) by having the opportunity to override some of the ExPERT database ground level values.

In order to select a variable, a checkbox has been inserted next to each of the variables' edit boxes. If the box is left unchecked, ExPERT LUT (Lookup Table) values will be used for the ground level values. If checked, the ExPERT LUT values will be overwritten. To safeguard against modifying a variable that already has a uniquely defined value, certain variables under certain conditions will become disabled. For instance, if the user entered ground level values for pressure, temperature, and dewpoint, the option to change the ground level values of specific humidity and saturation mixing ratio would become disabled. This is illustrated in Figure 4.

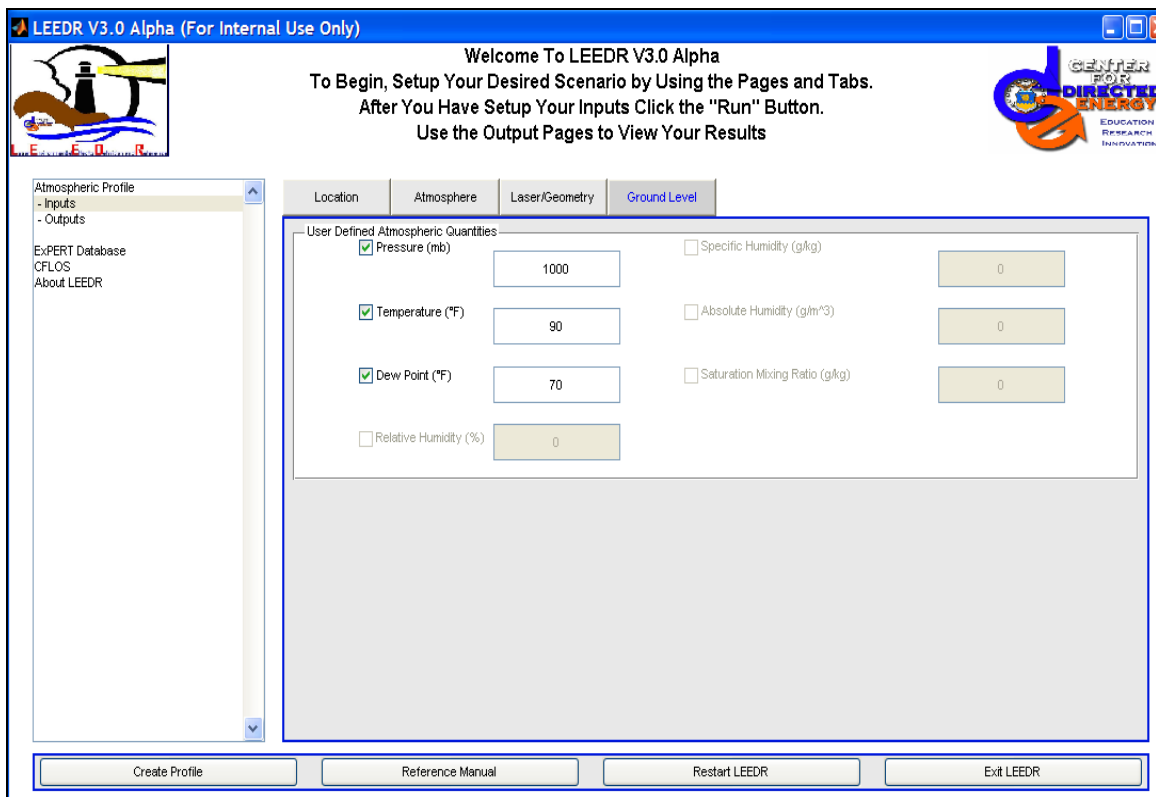


**Figure 4. User-Defined GUI Tab Safeguarding Technique**

Figure 4 depicts a situation in which pressure (mb), temperature ( $^{\circ}\text{F}$ ), and dewpoint ( $^{\circ}\text{F}$ ) have been chosen. The other variables, relative humidity, specific humidity, absolute humidity, and saturation mixing ratio, are disabled, due to their dependence on the previously modified pressure, temperature, and dewpoint.

After each ground level variable is defined, different methods based on the particular variable, are utilized in order to extrapolate the values throughout the boundary layer. In terms of pressure and temperature, the appropriate saturated or unsaturated lapse rate is used. Dewpoint and relative humidity are calculated based on the ground level temperature, as well as each variable's respective ground level value. After calculating the dewpoint, LEEDR is able to use the extrapolated dewpoint and temperature to determine the relative humidity. The Goff-Gratch equation [20:350] is used to convert dewpoint to vapor pressure and obtain other moisture parameters.

After calculating the pressure, temperature, dewpoint, and relative humidity, LEEDR is able to determine the absolute humidity, specific humidity, and saturation mixing ratio. For the case in which a user-defined absolute humidity, specific humidity, or saturation mixing ratio is not supplied, LEEDR uses the Goff-Gratch equation to initialize the computation of these variables. In summary, the Goff-Gratch equation with dewpoint as the variable produces the saturation vapor pressure. From the saturation vapor pressure, one can determine the saturation mixing ratio. One can then use the saturation mixing ratio to define the specific humidity, which can be used to compute the absolute humidity. If the user supplies a ground level absolute humidity, specific humidity, or saturation mixing ratio however, the saturation vapor pressure is determined by utilizing Bolton's equation [28]. Bolton's equation is defined as the following:

$$e_s(T_d) = 6.112 \exp\left(\frac{17.67T_d}{T_d + 243.5}\right) \quad (28)$$

where  $T_d$  is the *dewpoint* ( $^{\circ}\text{C}$ ), and  $e_s$  is the *saturation vapor pressure* (g/kg). Whereas the Goff-Gratch equation is accurate from  $-50^{\circ}\text{C} < T_d < 50^{\circ}\text{C}$ , Bolton's equation has been shown to be accurate for the following dewpoint range:  $-30^{\circ}\text{C} \leq T \leq 35^{\circ}\text{C}$ , which is acceptable for the calculations in LEEDR. After determining the saturation vapor pressure using Bolton's equation, the saturation mixing ratio, specific humidity, and absolute humidity are computed in the same manner as mentioned before (e.g. saturation mixing ratio is determined from the saturation vapor pressure, which is in turn utilized to calculate the specific humidity, etc.).

### **Correlated-k Binning Method**

The main focus of the Correlated-k section of this project is to speed up the transmission calculation time for a user-defined spectral interval, while retaining the near-continuous consideration of the spectral band of interest. This part of the project is accomplished in essence, by utilizing method similar to that used in Modtran.

Essentially, the user is able to perform path radiance calculations based on very small intervals of band-averaged transmittance, at the end of the user's path length. In summary,

“Modtran is a ‘narrow band model’ atmospheric radiative transfer code. The atmosphere is modeled as stratified (horizontally homogeneous), and its constituent profiles, both molecular and particulate, may be defined either using built-in models or by user-specified vertical profiles. The spectral range extends from the UV into the far-infrared (0-50,000  $\text{cm}^{-1}$ ), providing resolution as fine as 0.2  $\text{cm}^{-1}$ ” [1].

The Correlated-k section of this project is described as a three step process. First, the LEEDR program is run under a certain scenario, in order to obtain extinction



coefficients as a function of frequency. Once the extinction coefficients are determined, a Matlab script is used to save the coefficients in a flat-file database for the Correlated-k method. After the extinction coefficients are stored, a second Matlab script, which contains the Correlated-k method, performs one of two functions based on the user's inputs. If the user has not run the script previously (for the particular set of extinction coefficients), the script performs the Correlated-k method on the extinction coefficients, and stores the resulting  $k(g)$  points. If however, the user has run the script, and in turn determined the  $k(g)$  points, the script then by-passes the Correlated-k section, and solely compute the transmittance over the desired interval and path length.

The specific Correlated-k algorithm that was used for this project is depicted in the Liou text [9:127-137]. Figure 5 displays the method that Liou utilizes.

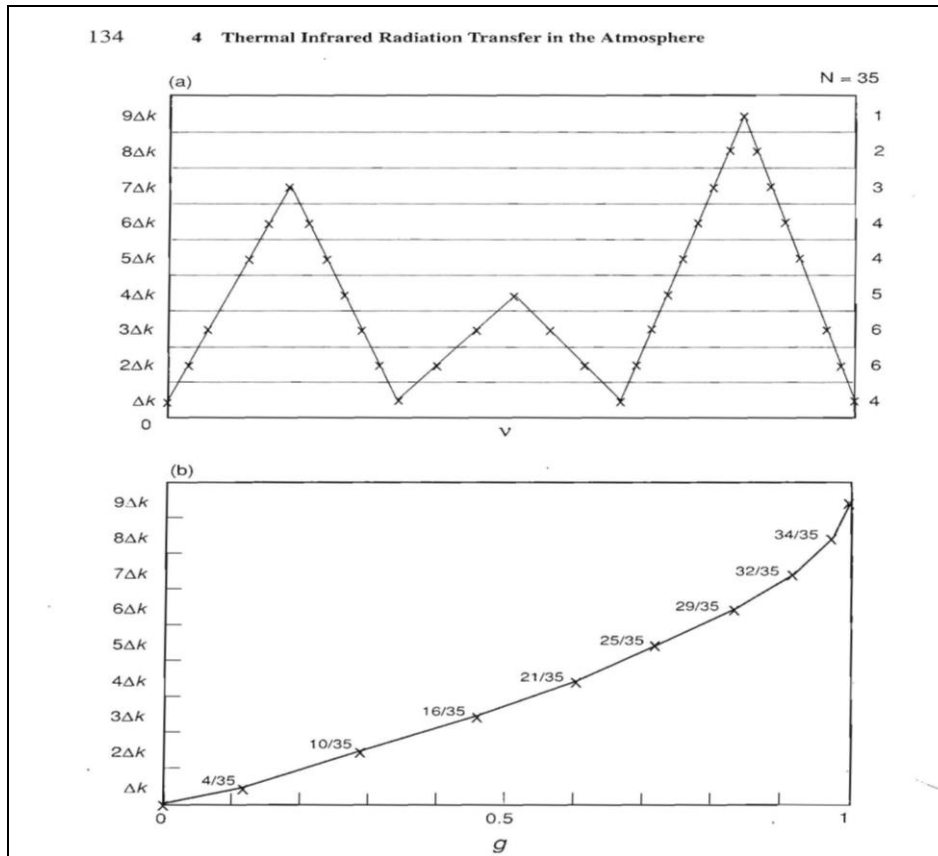


**Figure 5. Illustration of the mapping of the absorption coefficient from the  $v$ -domain to the  $g$ -domain. (a) Absorption coefficients of three lines in the  $v$ -domain and division of the  $k$ -space into 10 equal intervals. The numbers are the data points in each interval with a total number of 35. (b) By definition,  $g(j\Delta k) \equiv n(0, j\Delta k)/N$ ,  $j = 0, 1, \dots, 9$ . Thus, the data points in the  $v$ -domain are transformed to the  $g$ -domain, where  $g$  is a monotonic increasing function. (Courtesy of [9:134])**

The top graph (labeled (a) in Figure 5) represents a hypothetical extinction spectrum interval. For this particular example, there are 35 extinction points, ranging in value from 0 to  $9\Delta k$ . In order to begin the process of obtaining the corresponding  $k(g)$  points (referenced in equation 26), the extinction points are put, for example, in 10 different evenly spaced bins. The particular  $k(g)$  point is determined by summing the number of extinction points in a certain bin, as well as any extinction points in bins corresponding to lower extinction values, and dividing by the total number of extinction

points in the domain. Thus, for the first  $k(g)$  point corresponding to the region  $\Delta k$  in the top graph, there are 4 points in this bin, and 35 extinction points in the domain. The resulting  $g$  value for this bin would be  $g = 4/35$ . Although it was not specifically stated in Liou, the middle extinction value pertaining to the bin, was used for the corresponding  $k(g)$  point. Thus, for the first  $k(g)$  point,  $\frac{\Delta k}{2}$  would be the  $k(g)$  value for  $g = 4/35$ . The graph (b) in Figure 5 represents the end result of performing the calculations over all of the bins.

Mathematically, the Correlated- $k$  for homogeneous atmospheres (or  $k$ -Distribution method) calculates the cumulative probability in essentially one of two ways. By definition, the cumulative probability function is defined as:

$$g(k) = \int_0^k f(k) dk \quad (29)$$

where  $f(k)$  is the *probability distribution function* of the extinction points. Another way to calculate the cumulative probability distribution function, which is utilized for this project, is through the following equation:

$$g(k) = \frac{1}{\Delta \nu} \sum_j \int_0^k \left| \frac{\Delta \nu_j}{\Delta k} \right| dk' = \frac{1}{\Delta \nu} \sum_j \int_0^k \Delta \nu_j(k) = \frac{n(0, k)}{N} \quad (30)$$

Relating this back to Figure 5,  $n(0, k)$  is the *number of points in the particular bin as well as any lower bins*,  $N$  is the *total number of extinction points in the domain*, and  $j$  is the *particular absorption line being observed across the part of the spectrum  $\Delta \nu$*  (e.g. in Figure 5,  $j$  would vary from 1 to 3, since there are 3 peaks in the part of the spectrum). Thus, one is able to obtain a discrete number of  $k(g)$  points.

Once the  $k(g)$  points (or equation), have been determined, the optical depth can be defined. The optical depth, by definition is the amount of extinction, corresponding to a particular molecule (or group of molecules) that one encounters along an atmospheric path length. Mathematically, the optical depth is represented as:

$$\tau(z_1, z_2) = \int_{z_1}^{z_2} \beta_e(g, p, T) dz = \int_{z_1}^{z_2} \rho_i k_{e,i}(g, p, T) dz \quad (31)$$

where  $\tau$  is the *optical depth*,  $\beta_e$  is the *volume extinction coefficient* ( $\text{km}^{-1}$ ),  $\rho_i$  is the *mass density of a particular molecular absorber* ( $\text{kg}/\text{m}^3$ ), and  $k_{e,i}$  is the *mass extinction coefficient* ( $\text{m}^2/\text{kg}$ ). For the optical depth calculations in LEEDR, the following molecular absorbers (along with their respective mass extinction coefficients) are utilized:  $\text{H}_2\text{O}$ ,  $\text{CO}_2$ ,  $\text{O}_3$ ,  $\text{N}_2\text{O}$ ,  $\text{CO}$ ,  $\text{CH}_4$ ,  $\text{O}_2$ ,  $\text{NO}$ ,  $\text{SO}_2$ ,  $\text{NO}_2$ ,  $\text{NH}_3$ , and  $\text{HNO}_3$ . The resulting transmission value can then be found by referencing the appropriate equation (25-27).

For a homogeneous atmosphere, the optical depth equation can be modified. Due to the fact that pressure and temperature are essentially constant in a homogeneous atmosphere, the extinction coefficients can be factored out of the equation. Thus, for the case in which one has the volume extinction coefficient (which was the case for this project), the equation is reduced to the extinction coefficient multiplied by the path length. If, on the other hand, one has the mass extinction coefficient, the equation becomes the integral of the mass density of the particular absorber, multiplied by its respective extinction coefficient.

In order to compute the transmission in a homogeneous atmosphere for this project, a slight modification was made to equation 26. Equation 26, in essence,

computes the transmission by integrating (or summing) over the number of transmission points, over the  $g$  domain. The Riemann sum in particular, approximates the transmission over the  $g$  domain, by referencing a single value ( $e^{-k(g_i)u}$ ) across a certain section of the domain ( $\Delta g_i$ ). In regions of low extinction, this approximation works well. This is due in part to the small extinction difference between the top bin and lower bin (Figure 5a illustrates top and lower bins). Figure 6 and Figure 7 show an example spectral band where LEEDR depicts several weaker extinction lines, for a 1 km vertical path, from  $13163 \text{ cm}^{-1}$  to  $13167 \text{ cm}^{-1}$ .

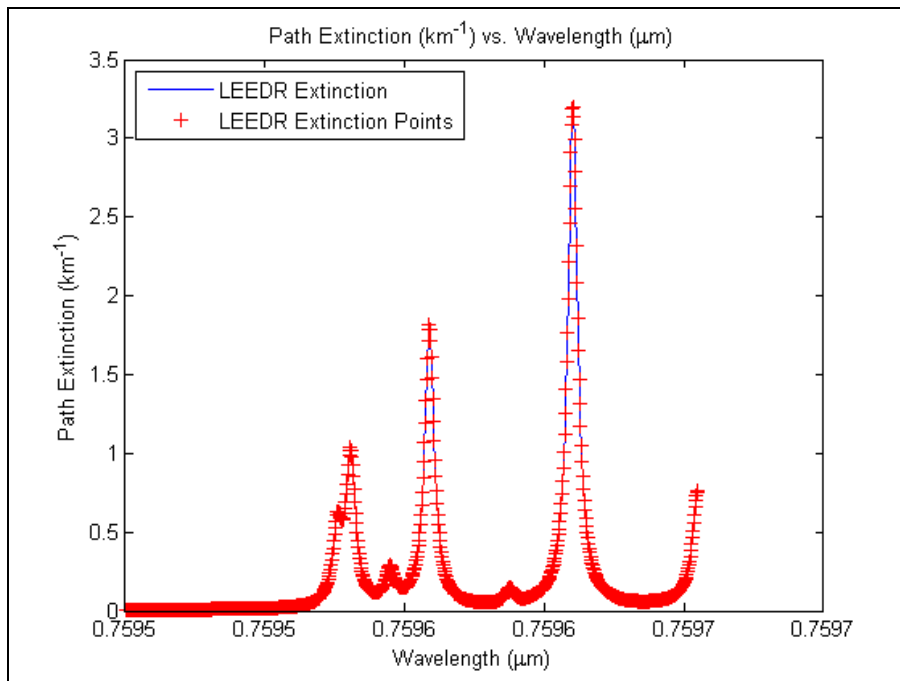


**Figure 6. Region of Low LEEDR Extinction**

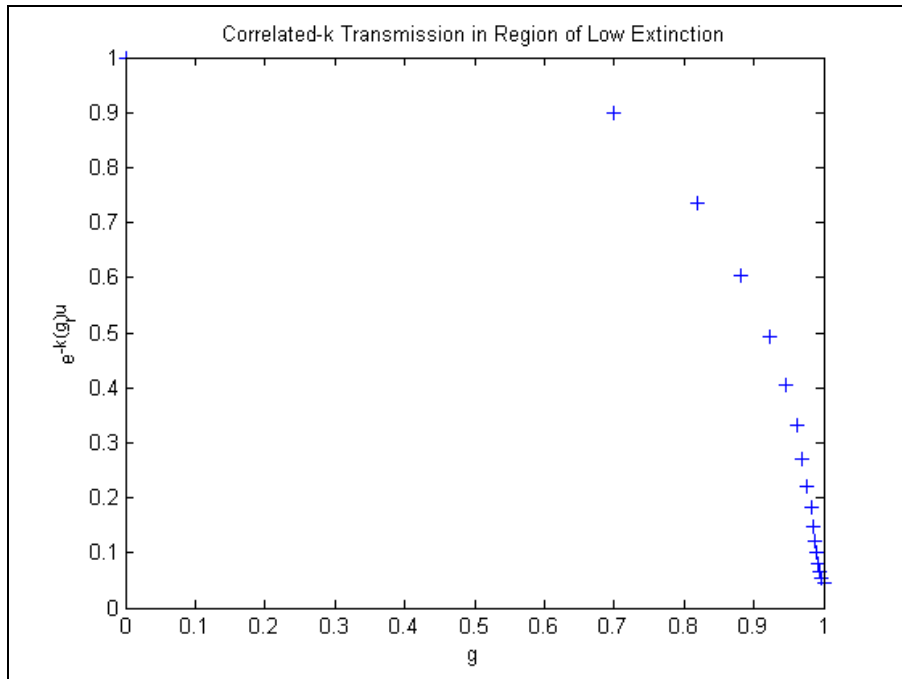


**Figure 7. Correlated-k Transmission in a Region of Low LEEDR Extinction**

As one can see in Figure 7, very little transmission is lost based on which  $e^{-k(g)u}$  point is chosen over a certain  $\Delta g$ . For this particular plot, one could lose a maximum of 20% transmission for one interval, based on the  $g$  point chosen. Comparing this example, to an interval containing higher extinction values, the need for a more appropriate transmission equation becomes apparent. Figure 8 and Figure 9 show an example spectral band where LEEDR depicts two relatively strong extinction lines, for a 1 km vertical path, from  $13131 \text{ cm}^{-1}$  to  $13135 \text{ cm}^{-1}$ .

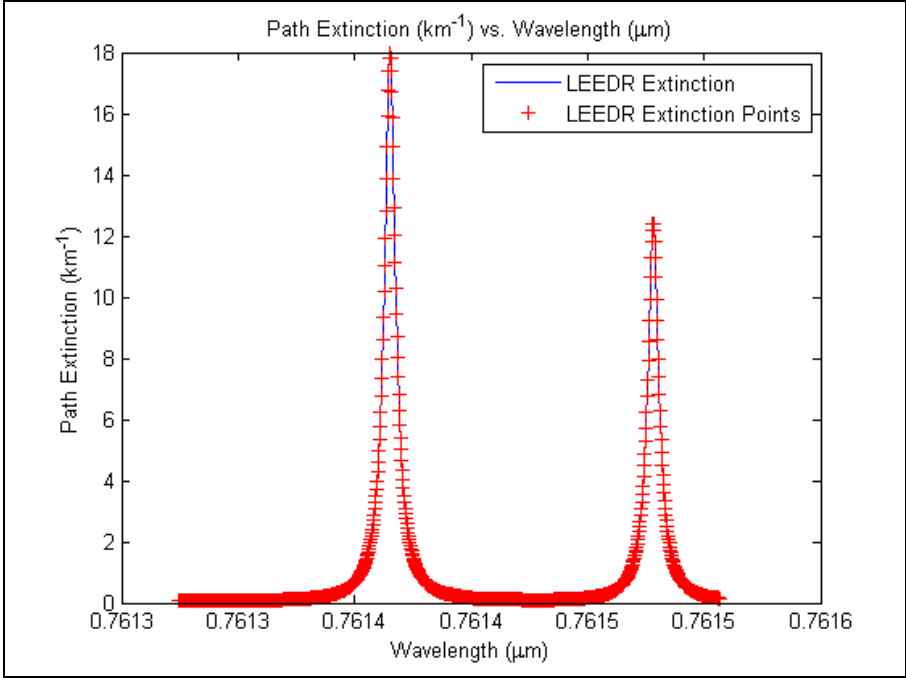


Figure 8. Region of High LEEDR Extinction

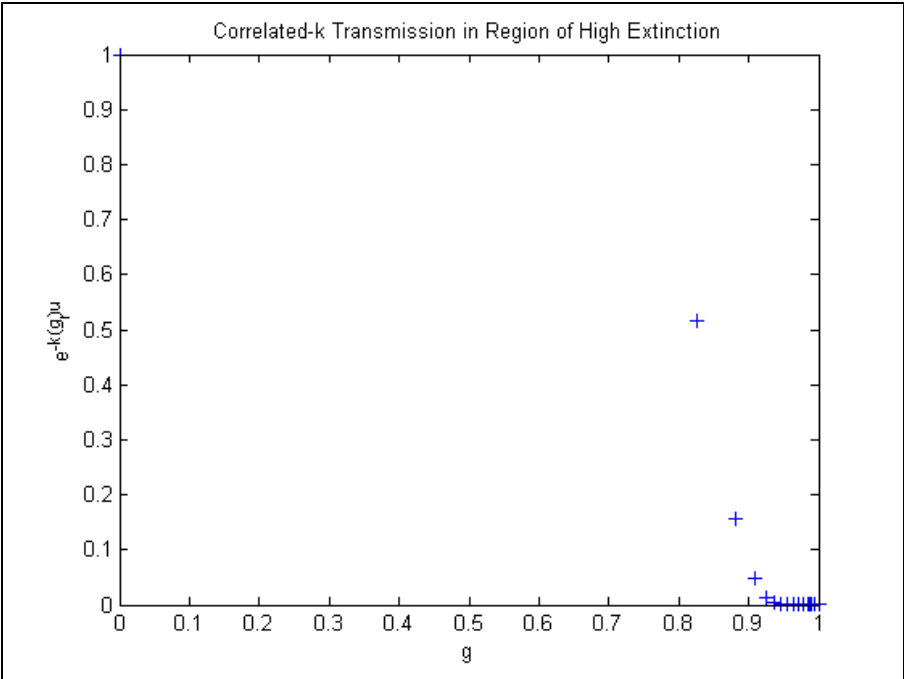


Figure 9. Correlated-k Transmission in a Region of High LEEDR Extinction

For the interval shown in Figure 8 and 9, the largest path extinction value is around  $18 \text{ km}^{-1}$ , whereas the previous interval (shown in Figure 6 and 7) did not contain any extinction value higher than  $3.5 \text{ km}^{-1}$ . Thus, as a result of the higher extinction, based on which  $k(g)$  point is selected, transmission differences for a single  $\Delta g$  interval can vary by  $\sim 50\%$ . In order to combat this problem, a trapezoid modification was utilized. As a result, equation 26 becomes:

$$T_{\bar{v}}(u) = \int_0^1 e^{-k(g)u} dg \cong \sum_{i=2}^M \Delta g_i \left( \frac{|e^{-k(g_i)u} - e^{-k(g_{i-1})u}|}{2} + e^{-k(g_i)u} \right) \quad (32)$$

By modifying equation 26, equal weight is given to each  $e^{-k(g)u}$  bound point for a particular subinterval  $\Delta g$ , and thus a better approximation of the transmittance is given over the entire wavelength interval.

In the case of realistic nonhomogeneous atmospheres, one does notice a dependence of the extinction coefficient on path length. Thus, one would need to be able to model the extinction coefficient as a function of altitude (rather than utilizing the local value), and compute the integral over a certain altitude. Based on the quantities that one is able to obtain, one can in turn modify the optical depth by noting that the mass density of the molecular absorber can be represented by its mixing ratio, and the air density. The resulting equation is:

$$\tau(z_1, z_2) = \int_{z_1}^{z_2} \beta_e(g, p, T) dz = \int_{z_1}^{z_2} k_{e,i}(g, p, T) q(z) \rho(z) dz \quad (33)$$

where  $\beta_e$  is the *volume extinction coefficient* ( $\text{km}^{-1}$ ),  $k_{e,i}$  is the *mass extinction coefficient* ( $\text{kg/m}^2$ ),  $q$  is the *mixing ratio* (defined as  $q = m_a/m$  where  $m_a$  is the *mass density of the molecular absorber* and  $m$  is the *mass density of the air*), and  $\rho$  is the *air density*



(defined as  $\rho = p/R_d T$  where  $p$  is *pressure* in Pa,  $R_d$  is the *gas constant of dry air* in  $\text{J K}^{-1} \text{kg}^{-1}$ , and  $T$  is *temperature* in K).

## IV. Analysis and Results

### Overview

This chapter focuses on the differences created in the boundary layer by the user-defined ground level GUI in LEEDR, as well as the time and accuracy variations observed between the Correlated-k scripts and the LBL method currently implemented in LEEDR. In terms of the user-defined ground level tab, modifications of ground level characteristics ultimately lead to deviation from the default LEEDR values. In addition, when compared to sounding data, the modified ground level values are shown to be more accurate than the climatological data, throughout the boundary layer, for a specific site and time. The Correlated-k algorithm on the other hand, enabled the user to compute a band representative transmittance by referencing  $4 \text{ cm}^{-1}$  intervals, while reducing computation time in comparison to the LBL algorithm.

### User-Defined Ground Level Input Tab

In order to provide an accurate test of the user-defined ground level GUI, the current version of LEEDR and the version with the ground level GUI are compared directly to an upper air sounding measurement. The ExPERT (climatological) site chosen from LEEDR for this part of the project is Wright-Patterson AFB, OH. The upper air sounding data is taken from the closest location with respect to the ExPERT location where a weather balloon is regularly launched for measurement. This site is Wilmington, OH, which is symbolized as ILN or KILN [18]. The particular date and time of day chosen is, 11 March 2004 at 1900L (00Z EST). The time (i.e. 00Z or 1900L) is selected due to its relation with the boundary layer. By choosing a late afternoon time (soundings are taken at 12Z and 00Z), one would encounter a larger boundary layer, and thus more

of a comparison could be made between the sounding data and the ground level modified LEEDR values. The date is selected due to its interpolated temperature value, with respect to the average Wright-Patterson AFB temperature for March. The average normal temperature for Dayton, OH, according to the National Weather Service's website [19], is 49.5 °F for March.

Table 1 lists all of the information that is utilized in order to compute the LEEDR atmosphere. The first section, entitled "Conditions from Upper Air Sounding", lists the measurements that were obtained from the upper air sounding website at the lowest recorded altitude (which was 317 m), corresponding to the previously defined location and time. The second section, entitled "LEEDR Data" lists the inputs that are entered into the LEEDR program in order to model atmospheric conditions on March 11, 2004 at 00Z.

**Table 1. LEEDR Data without Ground level Modification**

<b>Conditions from Upper Air Sounding</b>		
Upper Air Sounding Location:	Location: Wilmington, OH (ILN)	Latitude: 39.428 °N
		Longitude: 83.792 °W
		Elevation: 317 m
Pressure:	986 mb	
Temperature:	45.32 °F	
Dewpoint:	18.32 °F	
Relative Humidity:	34 %	
<b>LEEDR Data</b>		
Location Tab:	Current Location:	Latitude: 39.83 °N
		Longitude: 84.05 °W
		Elevation: 251 m
	Nearest ExPERT Site:	Dayton/Wright-Patterson
	Season:	Winter
	Time of Day:	1800-2100
	Percentile of Relative Humidity:	50 <sup>th</sup> Percentile – Median (Average)
	Atmosphere:	ExPERT Atmosphere
	Molecular Effects Model:	Calculations
	Aerosol Effects Model:	GADS Worldwide Aerosols
LEEDR Atmosphere Tab:	Turbulence Model:	HV 5/7
	Wind Model:	Climatological Wind Profile
	Clouds/Rain	None
LEEDR Laser/Geometry Tab	Laser Settings:	Wavelength: 1.31525 µm
	Vertical Path:	Upper Altitude: 2000 m
		Lower Altitude: 0 m
Ground Level Tab:	Pressure:	986 mb
	Temperature:	45.32 °F
	Dewpoint:	18.32 °F

All of the values in the section “LEEDR Data” of Table 1 are selected based on their closest match to the date and time of the upper air data. For example, the time chosen for this atmosphere is 1800-2100. This is the closest match that could have been selected, in response to the upper air measurement time of 00Z or 1900L. Based on the

way that LEEDR is configured, the user can only select a time interval of 3 hours for an ExPERT atmosphere. The relative humidity percentile selected is the 50<sup>th</sup> percentile because this is most representative for “average” conditions. So, the lowest elevation pressure, temperature, and dewpoint from the sounding are entered into LEEDR through the ground level GUI, and a comparison is made where the LEEDR data and the sounding data are started at an elevation of 0 m.

After compiling both atmospheric profiles, the variations observed in pressure, temperature, dewpoint, and relative humidity are show in Figure 10. The relative humidity profiles are calculated from the pressure, temperature, and dewpoint.

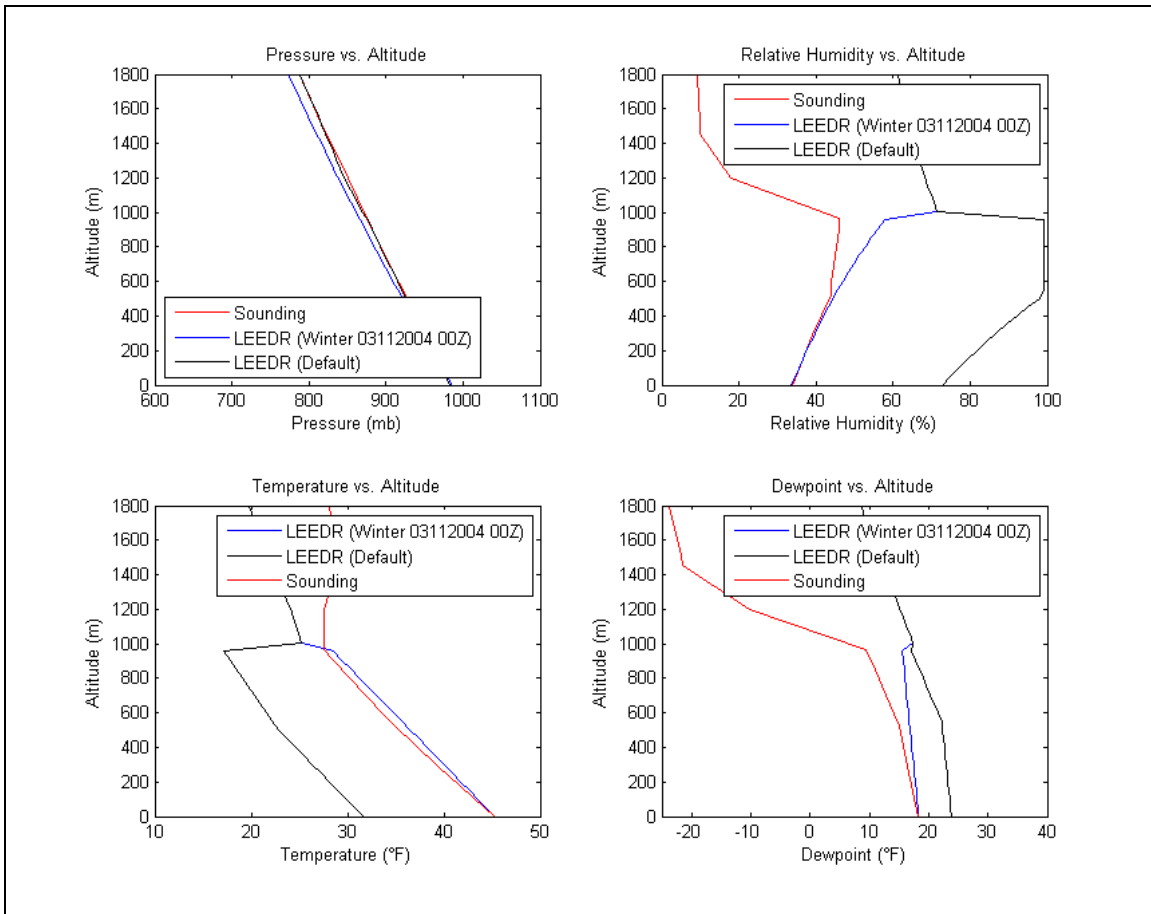


**Figure 10. Variation Observed in LEEDR Output Variables based on Ground Level Modification**

Figure 10 displays the upper air sounding data, “LEEDR (Winter 03112004 00Z)” ground-modified, and “LEEDR (Default)” EXPERT database ground level data, at the altitude of the lowest sounding (i.e. 0 m corresponds to the lowest sounding altitude). When compared to the sounding data, one notices a much better correlation between the modified ground level data and the upper air sounding data, within the boundary layer. Also of note, is how well the LEEDR ground level GUI “predicts” the height of the boundary layer (which was 1000 m for the LEEDR data, and 1031 m for the upper air sounding) and the temperature variation within it. Above the boundary layer, as is shown

in Figure 10, the ground-modified LEEDR values merge with the ExPERT database and values.

### Correlated-k Algorithm Development

In order to test the Correlated-k script for a homogeneous atmosphere, the following scenario shown in Table 2, is used in LEEDR.

**Table 2. LEEDR Defined Atmosphere for Correlated-k Method**

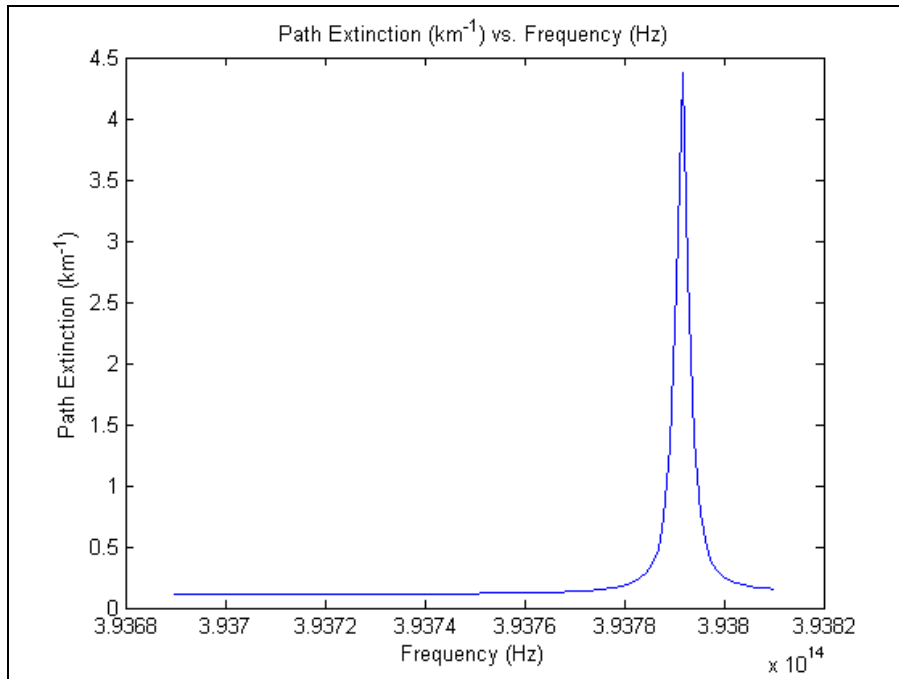
<b>Location Tab</b>		
Current Location:	Type:	Land
	Latitude:	39.83
	Longitude:	-84.05
Nearest ExPERT Site:	Dayton/Wright-Patterson AFB	
	Latitude: 39.83	39.83
	Longitude: -84.05	-84.05
Season	Summer	
Time of Day:	1200-1500	
Relative Humidity :	50 <sup>th</sup> Percentile – Median (Average)	
Atmosphere:	ExPERT Atmosphere	
Molecular Effects Model:	Calculations	
Aerosol Effects Model:	Clear (No Aerosols)	
<b>Atmosphere Tab</b>		
Turbulence:	Turbulence Model:	HV 5/7
Wind:	Wind Model:	Climatological Wind Profile
Clouds/Rain:	None	
<b>Laser/Geometry Tab</b>		
Laser Settings:	Wavelength: 1.31525 $\mu\text{m}$	1.31525um
Geometry Settings:	Vertical Path:	Upper Altitude (m): 0
		Lower Altitude (m): 1000

As indicated in Table 2, only molecular absorbers are present (i.e. no aerosols, cloud droplets, or rain droplets). This enables faster extinction calculations over a user-

defined interval, due to the fact that LEEDR does not have to calculate absorption and scattering from cloud droplets and aerosols. This in turn enables one to obtain extinction points with unique extinction coefficients for the Correlated-k method, over a larger section of the domain. The larger number of extinction points allows one to obtain a better understanding of how the transmission calculated from the Correlated-k method coincides with the transmission derived from the LBL method.

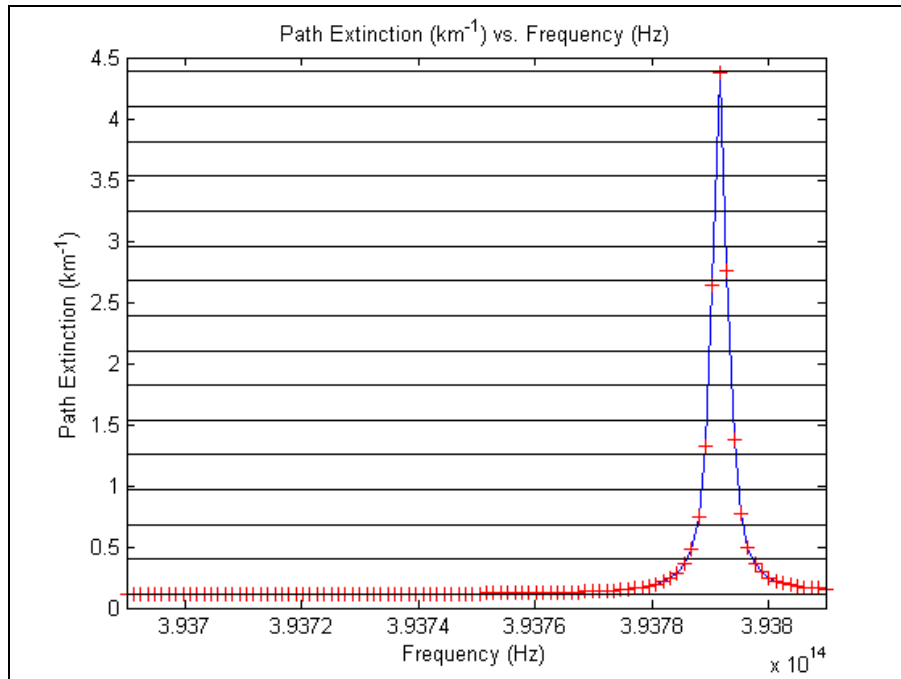
In order to accurately model the transmission in the previously defined homogeneous atmosphere, extinction coefficients are obtained on  $4 \text{ cm}^{-1}$  intervals. Once obtained, the extinction coefficients are binned, in evenly spaced bins across the  $4 \text{ cm}^{-1}$  domain. After binning the extinction coefficients, the corresponding  $k(g)$  points are determined, using equation 30. After determining the  $k(g)$  points, equation 26 is used to compute the band-averaged transmission over the  $4 \text{ cm}^{-1}$  interval. Figures 11-14 provide a conceptual model that illustrates the process that is used for this project to obtain the Correlated-k band-averaged transmission for a  $4 \text{ cm}^{-1}$  interval. The particular interval  $13123 \text{ cm}^{-1}$  to  $13127 \text{ cm}^{-1}$  is presented, under the atmospheric conditions presented in Table 2.





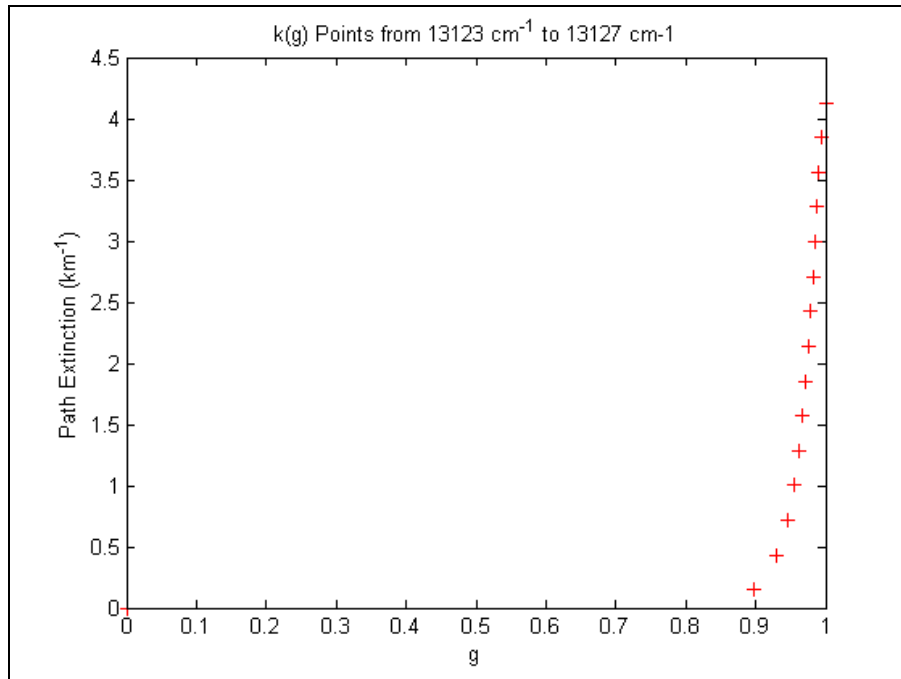
**Figure 11. LEEDR Extinction Coefficients Obtained for Correlated-k Process**

Figure 11 represents a plot of extinction versus frequency, obtained directly from LEEDR. One hundred equally spaced points were used to derive the extinction values over the 1 km vertical path over the 4 cm<sup>-1</sup> spectral interval.



**Figure 12. Binned LEEDR Extinction Coefficients**

The red crosses shown in Figure 12 represent extinction data that is received directly from the LBL calculation method in LEEDR. For this particular figure, 100 points were analyzed over the  $4 \text{ cm}^{-1}$  interval. The black lines represent the bin edges that were used for this project. The blue lines in turn, represent LEEDR connecting the discretely sampled extinction points. Note that no LEEDR data is available in this case, between the red crosses. Also, for the Correlated-k method used in this project, 15 evenly spaced bins are utilized. The ultimate choice of 15 evenly spaced bins is based upon the transmission differences that are observed for differing bin sizes.



**Figure 13. Resulting  $k(g)$  Points for Correlated-k Method**

In reference to Figure 13, each of the red crosses represents the cumulative sum from the bins corresponding to lower extinction, to higher extinction (from  $g = 0$  to  $g = 1$ ). Figure 12 and Figure 13 represent the Correlated-k method applied to this spectral interval as is demonstrated by Liou in Figure 5a and 5b.

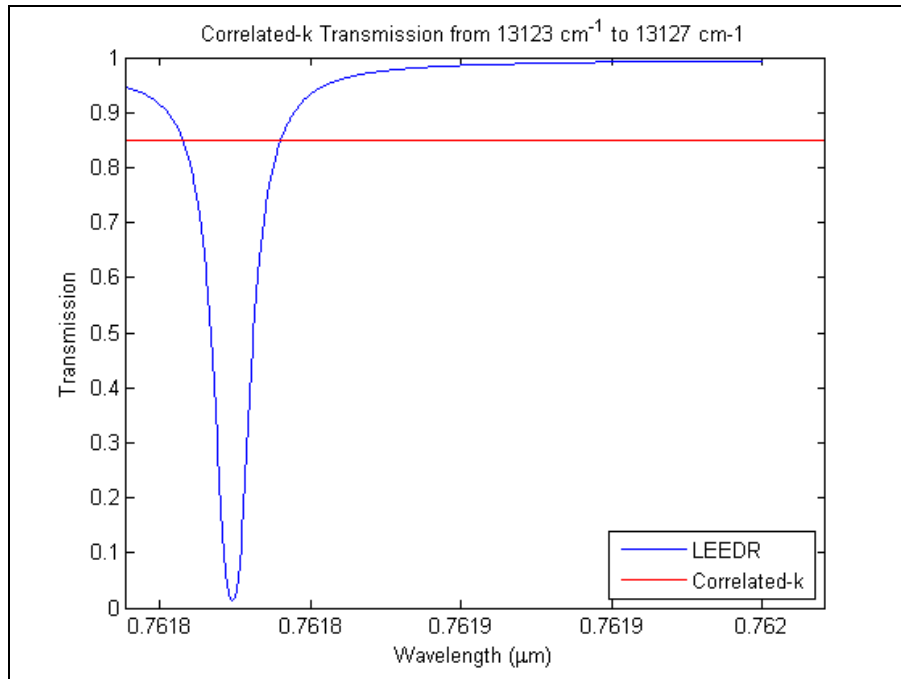


**Figure 14. Band-Averaged Correlated-k Transmittance for 4 cm<sup>-1</sup> Interval**

Figure 14 represents the end result of the Correlated-k process for a single 4 cm<sup>-1</sup> interval. The result is a band-averaged transmission value, for the entire interval. The transmission value displayed here however, is only a small portion of what would be displayed to the user. Ultimately, for a user-defined interval (which will consist of multiple 4 cm<sup>-1</sup> intervals), the band-averaged transmission values will be appropriately weighted (in terms of boundary conditions in which the user's interval references a portion of a 4 cm<sup>-1</sup> interval in the database), and displayed to the user.

Currently, the Correlated-k process is a stand-alone process (it is not currently incorporated into LEEDR). In order to automate the Correlated-k process depicted in previous Figures 11-14, two Matlab scripts are used. The first script stores the LEEDR extinction coefficients over the 4cm<sup>-1</sup> intervals, in a flat-file database. A typical database

file of extinction coefficients includes the frequency (Hz) in the first column, and the corresponding extinction coefficients in the subsequent columns. A second Matlab script is used to perform one of two functions. The script either performs the Correlated-k binning method, or computes the transmission over the specified part of the domain and path length.

The second script initially prompts the user for an extinction coefficient database. Assuming the user has not run the script previously, the user in turn selects the appropriate extinction coefficient database. The user then is then prompted for a database consisting of  $k(g)$  points. Once again, assuming the user has not run the script previously, the user does not provide a  $k(g)$  point database. Subsequently, the user is prompted to enter the path length and domain. After entering the path length and domain, the extinction coefficients from the database, corresponding to user's specified domain and path length, are used in the Correlated-k binning method. Once the  $k(g)$  points are determined, the script prompts the user to save the  $k(g)$  points in a different flat-file database. By saving the  $k(g)$  points in a database, the user can supply them to the script (via the second prompt), by-pass the Correlated-k binning method, and compute the transmittance.

### Transmission Calculations

In order to ensure the validity of the Correlated-k method used in this project to the reader, the hypothetical spectrum that was presented in the Methodology section (Figure 5) is reproduced by passing the following extinction spectrum, into the Correlated-k script. Thus Figure 5a is recreated in Figure 15.

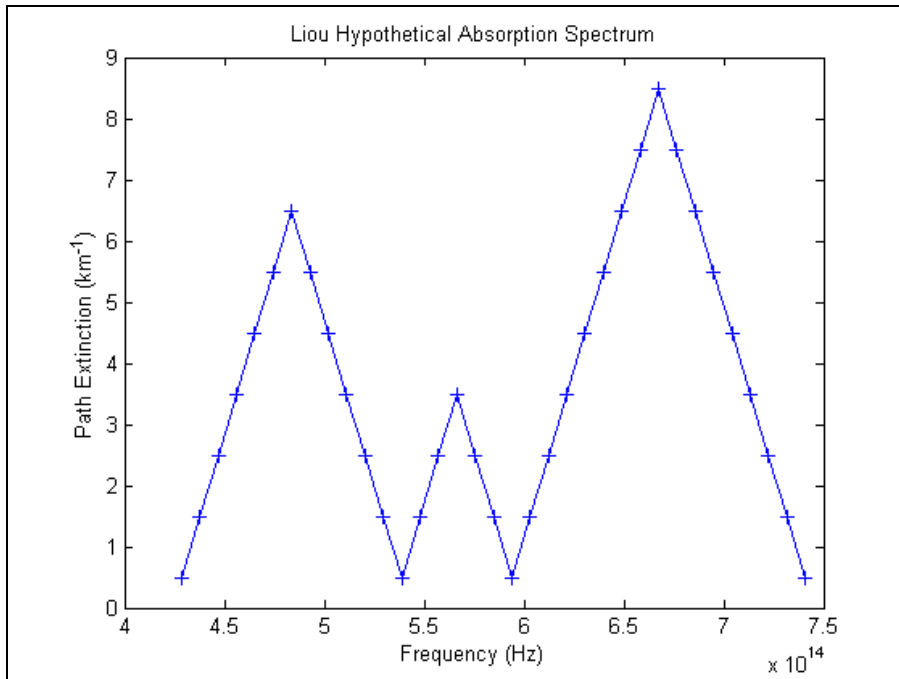


**Figure 15. Hypothetical Extinction Spectrum (Courtesy of Liou [9:134])**

In order to obtain the  $g$  values for Figure 15, extinction is assumed to vary from  $0 \text{ km}^{-1}$  to  $9 \text{ km}^{-1}$ , in increments of  $1 \text{ km}^{-1}$ . The resulting  $k(g)$  values are inserted in the middle of each axis marker of Figure 16.

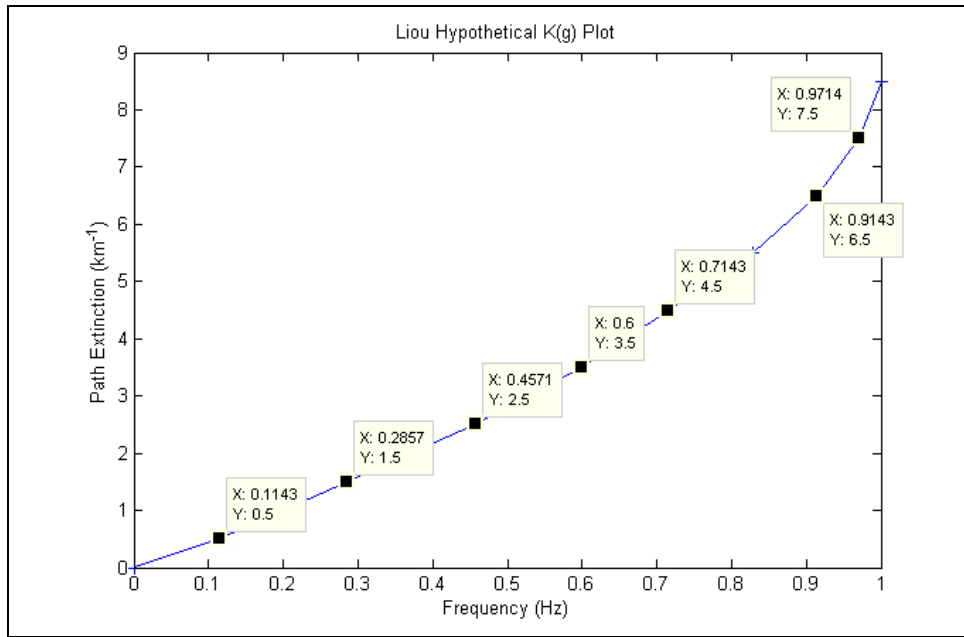


**Figure 16. Hypothetical k(g) Plot Produced from Correlated-k Script**

Figure 16 shows that the resulting k(g) values from the Correlated-k script coincide perfectly with those presented in the text [9:134] and Figure 5b.

With this understanding of the production of the k(g) points, the Correlated-k transmission can now be compared to a broader spectral band LBL output from LEEDR. Figure 17 illustrates accuracy that one can obtain with LEEDR, by using a similar amount of k(g) points as the Correlated-k method (i.e. 165 LEEDR points. The current Correlated-k method encompasses eleven  $4\text{cm}^{-1}$  intervals from  $13123\text{ cm}^{-1}$  to  $13167\text{ cm}^{-1}$  with 15 bins or k(g) points each).

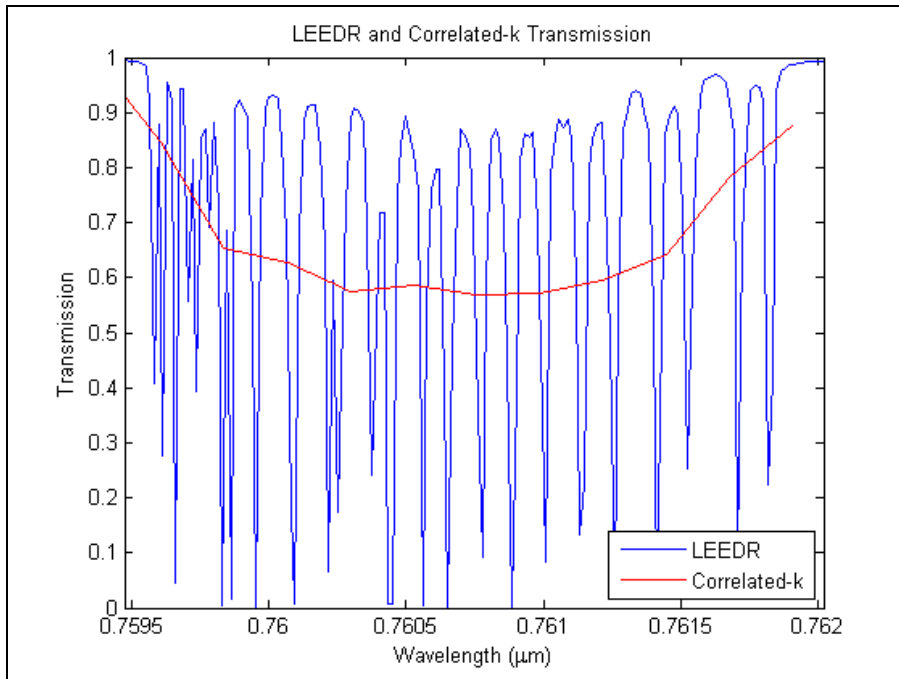


**Figure 17. Accuracy Comparison between Correlated-k and LEEDR Transmission**

While the LEEDR LBL output shown in Figure 17 displays far more detail in terms of peaks and minima of transmission than the Correlated-k line, much more computation time is required. In order to obtain the LEEDR transmission plot in Figure 17, one has to wait, on average, for 7 minutes (more discussion concerning computation time will be presented in the subsequent section). The Correlated-k transmission plot however, took on average, 35 seconds, after the  $k(g)$  database was constructed.

Figure 18 illustrates the adverse effects of trying to obtain LEEDR LBL results in the same amount of computation time as the Correlated-k method. The shorter computation time limits how many points across the interval where the LEEDR LBL calculation can be completed, thus leaving much of the spectral band unaccounted for.



This highlights a major advantage that the Correlated-k offers: near-continuous consideration of each spectral band of interest.

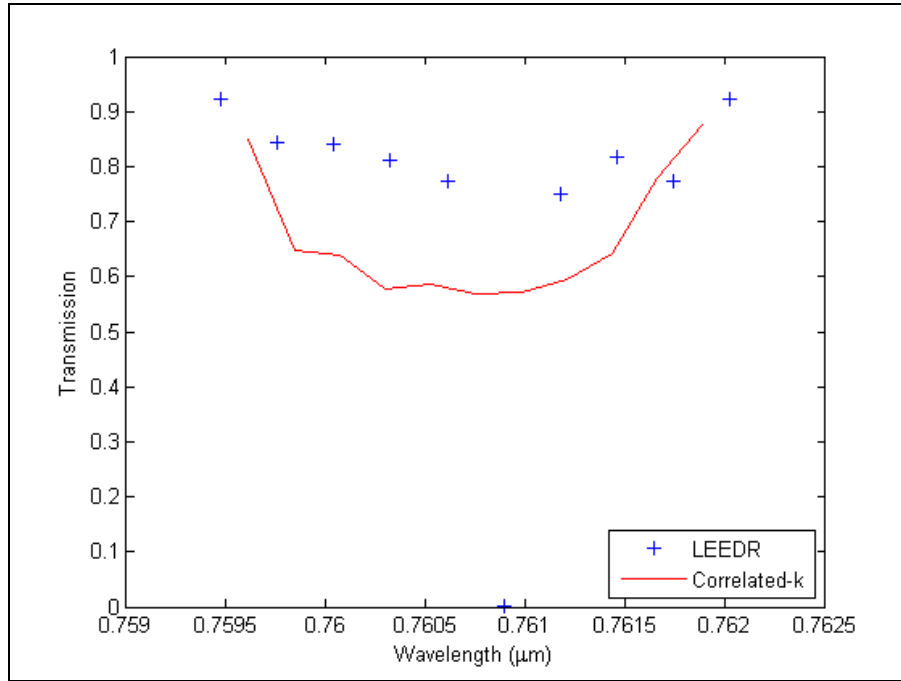


**Figure 18. Transmission Differences resulting from a Similar Correlated-k and LEEDR Run-time**

The LEEDR plot for Figure 18 took, on average, took 48 seconds to compute (10 points).

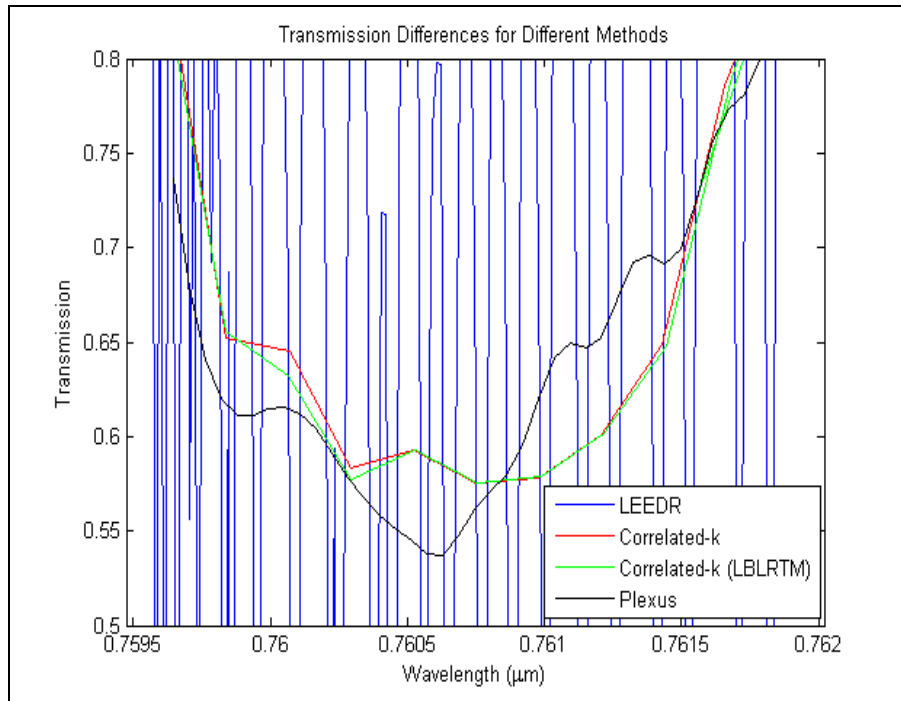


**Figure 19. Transmission Values for LEEDR, Correlated-k, Correlated-k (with LBLRTM), and Plexus from  $13123\text{ cm}^{-1}$  to  $13167\text{ cm}^{-1}$**

Figure 19 makes a comparison among several radiative transfer methods across the interval  $13123\text{ cm}^{-1}$  to  $13167\text{ cm}^{-1}$ . The “Plexus” line refers to a  $4\text{ cm}^{-1}$  interval Modtran 4.0 Correlated-k output. Plexus is an Air Force Research Lab (AFRL) GUI that runs Modtran 4.0. The LBLRTM [16] line is a Correlated-k output based on 190,000 point LBL output supplied by the LBLRTM model. The “LEEDR” and “Correlated-k” output in this case, is the same transmission data that is represented in Figure 17. Note the similarities between the Correlated-k lines derived from LEEDR and LBLRTM.

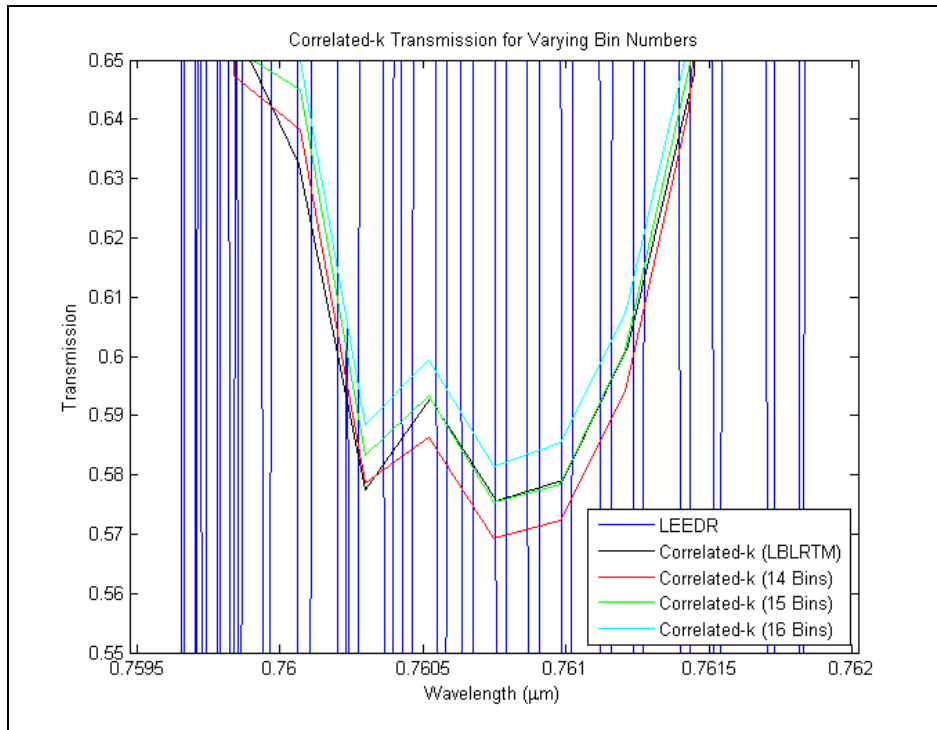


**Figure 20. Correlated-k Transmission with Varying Bin Numbers**

Figure 20 displays a variety of Correlated-k transmission values calculated by varying the number of evenly spaced bins encasing the extinction points. The previous figure has been inserted to reinforce the reasoning for choosing 15 bins, for each  $4 \text{ cm}^{-1}$  interval. As was discussed for the previous figure (Figure 19), the Correlated-k transmission with LBLRTM contained 190,000 extinction points across the  $13123 \text{ cm}^{-1}$  to  $13167 \text{ cm}^{-1}$  interval. Due to the number of points, as well as the method utilized to obtain the extinction points, the Correlated-k with LBLRTM correction or “Correlated-k (LBLRTM)”, can be assumed to provide the most accurate representation of the transmission. In Figure 20, the Correlated-k transmission algorithm was run under three different bin numbers (14, 15, and 16 bins). As is shown in the figure, the Correlated-k

line associated with 15 bins, correlates more closely to the LBLRTM line, and can thus be assumed to be the most accurate Correlated-k method with LEEDR extinction points.

Based on the previous description of the Correlated-k method however, one would expect the Correlated-k transmission to converge as the number of bins is increased. The reasoning for this is due in part to the fact that as more and more bins are used, the spacing in each bin decreases, and thus fewer points would be captured by any particular bin. Thus, when computing transmittance, less deviation would be observed due to the lack of variation in  $k(g)$  points. The lack of convergence that is shown in Figure 20 however, appears to be due to an under sampling issue. In order to create the Correlated-k transmission (with the exception of the Correlated-k with LBLRTM extinction values in Figure 20), 100 extinction points were utilized across the wavelength interval. In order to investigate the possibility of an under sampling error, LEEDR was run for 10,000 points over the interval  $13123 \text{ cm}^{-1}$  to  $13167 \text{ cm}^{-1}$ . Notably, with the additional sampling, the 10,000 point extinction data, the bin size that provided the best match to the LBLRTM Correlated-k line was the 15 point bin size. Thus, the 15 point bin size is considered optimal.

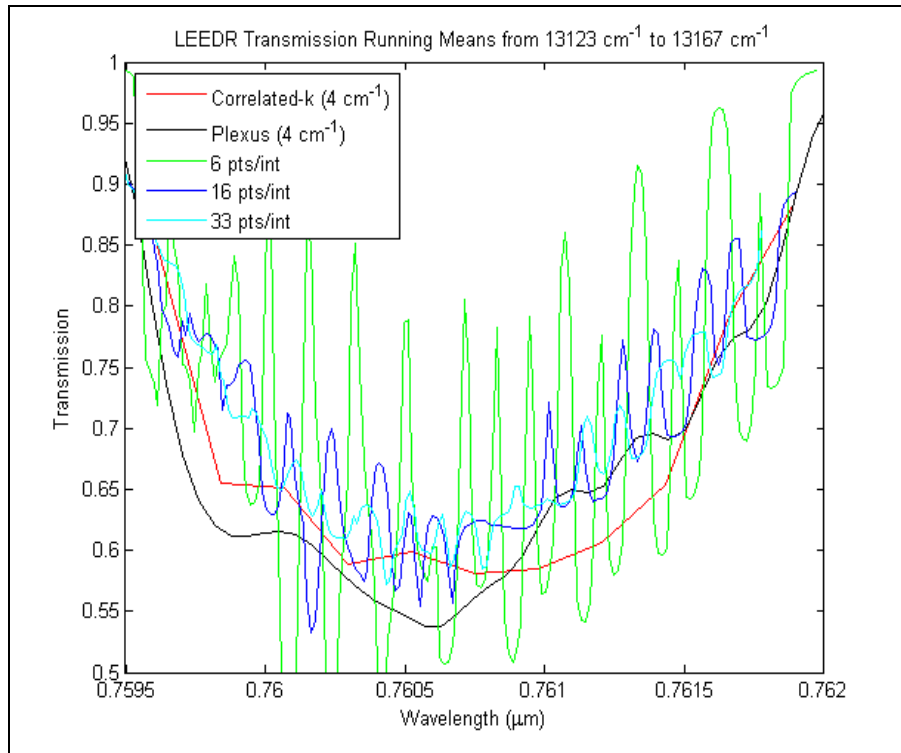


**Figure 21. LEEDR Transmission Running Means with Correlated-k Transmission**

Another way to check if the Correlated-k method is providing reasonable values is to compare it to a running mean. Figure 21 shows several running means based on the LEEDR 10,000 point LBL output compared to the Plexus and Correlated-k. For this particular figure, a constant window width was utilized, along with the midpoint for the window's domain. What the running mean allows one to observe is the trend of the data, while retaining the area under the curve. As one can see from Figure 21, as the window size increases, the smoothed out LEEDR transmission overlaps the Correlated-k transmission. The overlapped transmissions, (that in turn, have a similar area under the curve) are what one would expect to see utilizing the running mean method.

The reason for utilizing the running mean can be explained by the way each method is constructed. The LBL algorithm is very thorough, and thus one is able to observe a lot of detail, with respect to individual absorbers. In a typical LBL spectrum, one can observe numerous P- and R- branches corresponding to vibrational and rotational transitions. The Correlated-k algorithm however, calculates band-averaged transmission by referencing the distribution of extinction coefficients, typically from LBL calculations. As a result of creating a cumulative average of extinction coefficients and in turn calculating the  $k(g)$  points, the average extinction value changes between the wavenumber or frequency domain, and the  $g$  domain. The running mean inherently assumes that two methods have the same average for the dependent variable.

The previous comments can be summed up by noting the assumption that is made between for the Correlated-k method (equations 23 and 24) in the Methodology section. In order to transfer from the wavenumber or frequency domain, to the  $g$  domain, the following is assumed:

$$T_{\tilde{\nu}}(u) = \int_{\Delta\nu} \exp\left(-\int_u k_{\nu} du\right) \frac{d\nu}{\Delta\nu} = \int_0^1 \exp\left[-\int_u k(g) du\right] dg \quad (34)$$

Thus, in order to observe the same transmission values between the LBL and Correlated-k methods, one must ultimately have the same averaged extinction coefficients ( $k(g)$  and  $k_{\nu}$ ). The process is further illustrated through the following figures (Figures 22-24):

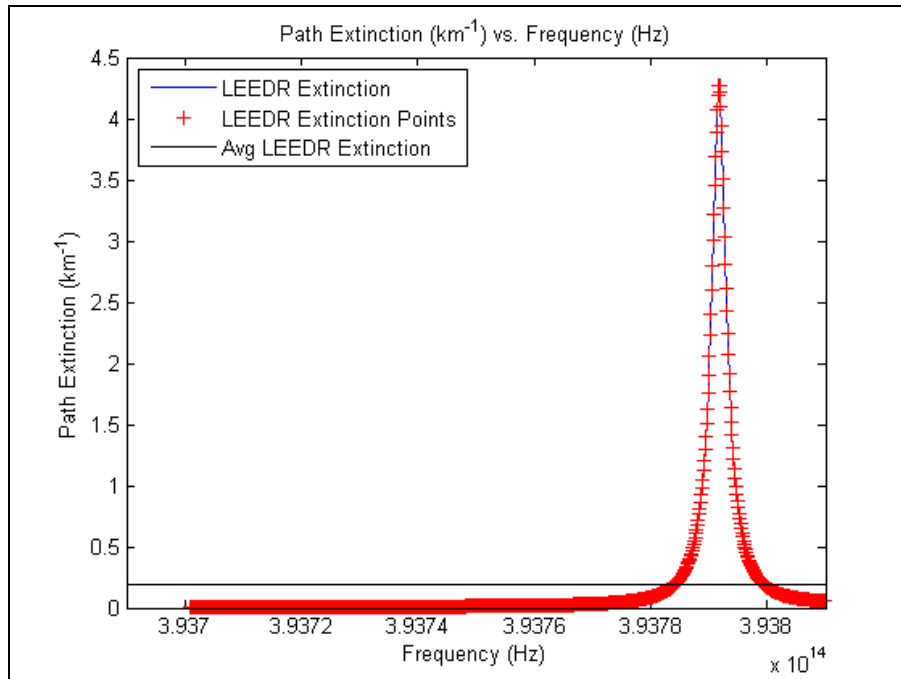


**Figure 22. Average LEEDR Extinction from 13123  $\text{cm}^{-1}$  to 13127  $\text{cm}^{-1}$**

Figure 22 displays the LEEDR extinction points that are obtained through a sample  $4 \text{ cm}^{-1}$  interval, as well as the average extinction value  $k_v$ . In essence, the black line displays the representative LEEDR or LBL extinction, across the interval.

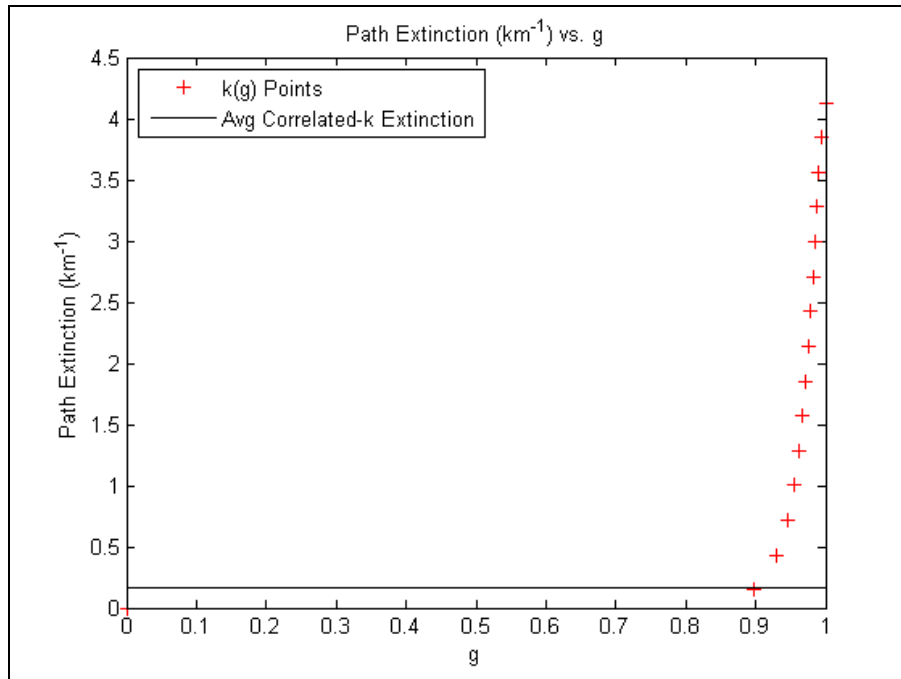


**Figure 23. Average Correlated-k Extinction from 13123  $\text{cm}^{-1}$  to 13127  $\text{cm}^{-1}$**

Figure 23 represents the average Correlated-k extinction  $k(g)$ , after the extinction has been transformed from the frequency domain, to the  $g$  domain. Figure 24 overlays the Correlated-k average extinction onto the previous LEEDR extinction plot (Figure 22).



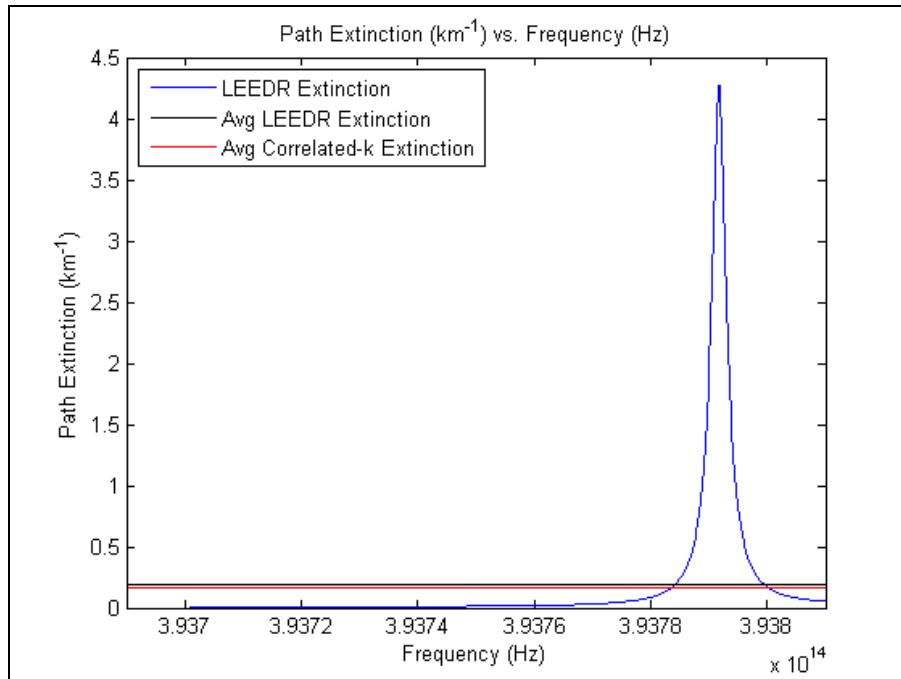


**Figure 24. Average LEEDR and Correlated-k Extinction from 13123  $\text{cm}^{-1}$  to 13127  $\text{cm}^{-1}$**

As one can see in Figure 24, the two average extinction values nearly coincide. The average extinction that was calculated for the Correlated-k method in the g domain is  $0.1628 \text{ km}^{-1}$ , while the average extinction for the LBL method in the frequency domain is  $0.1962 \text{ km}^{-1}$ . Based on the overlapping transmission values of the two methods, this is what one would expect.

In addition to the LEEDR running means and Correlated-k transmission that are displayed in Figure 21, transmission values computed from the radiative transfer program Plexus, using a Modtran transmission algorithm, was presented. In theory, the Correlated-k method, and the Plexus transmission curves, should match. On average however, one does notice slight differences. Throughout the entire interval, Plexus was

able to calculate a transmittance of 0.683. The Correlated-k method, on the other hand, computed an average transmittance of 0.677.

The previously discussed transmission differences between the Correlated-k and Plexus can be explained by noting the databases that each method utilizes to compute transmittance. The Plexus program uses the HITRAN98 database [23], while the LEEDR program (with LBL calculation algorithm) relies on HITRAN2004 [23]. In terms of the particular part of the spectrum observed by the Correlated-k method, line parameters corresponding to O<sub>2</sub> were updated for the 2000 and 2004 versions of the HITRAN database. From the 1998 version to the 2000 version in particular, “The Atmospheric A band, between the ground electronic state  $X^3\Sigma_g^-$  (with vibrational level  $v = 0$ ) and electronic state  $b^1\Sigma_g^-$  (with vibrational level  $v = 0$ ), centered at 0.76  $\mu\text{m}$ , has been revised...”[24]. The previously mentioned update to HITRAN could potentially describe the differences in transmission between the Plexus and Correlated-k methods.

### Calculation Times

In order to compute the Correlated-k transmission, the extinction coefficients had to be inserted into the appropriate database, and subsequently referenced by another script. The following run times correspond to six different intervals along the previously mentioned 13123  $\text{cm}^{-1}$  to 13167  $\text{cm}^{-1}$  interval:

**Table 3. Correlated-k Run Times to Compile Extinction Coefficient Database**

Interval (cm <sup>-1</sup> )	Run Times (seconds):
13123 to 13127	39
13127 to 13131	21
13131 to 13135	16
13135 to 13139	20
13139 to 13143	19
13143 to 13147	20

The extinction database script on average, took 23 seconds  $\pm$  8 seconds to store the coefficients. For the most part, similar times were recorded for each interval. One does however, notice one outlier. The first time recorded lies 16 seconds away from the mean run time. This can ultimately be attributed to an extra GUI prompting the user for the location and name of the new database.

The second script was analyzed for two different run times, since it served two purposes. The functions of this script were to produce a k(g) point database, as well as compute the transmission. In order to compile the database of the k(g) points, the following times were observed:

**Table 4. Correlated-k Run Times to Produce k(g) Database**

Interval (cm <sup>-1</sup> )	Run Times (seconds):
13123 to 13127	35
13127 to 13131	44
13131 to 13135	36
13135 to 13139	40
13139 to 13143	45
13143 to 13147	31

The average run time to compile a  $4 \text{ cm}^{-1}$  of  $k(g)$  coefficients was 39 seconds, with a standard deviation of 5 seconds.

The previous two tables display a portion of the entire  $k(g)$  point database that has been compiled. Presently, the database spans thirty-three  $4 \text{ cm}^{-1}$  intervals, from  $13123 \text{ cm}^{-1}$  to  $13167 \text{ cm}^{-1}$ . In order to provide a comparison however, between the transmissions calculation times using the Correlated-k method, verses the LBL method in LEEDR, transmission calculation times will be compared over the entire  $13123 \text{ cm}^{-1}$  to  $13167 \text{ cm}^{-1}$ . The following calculation times were observed using the Correlated-k method, after the  $k(g)$  database had been compiled:

**Table 5. Correlated-k Transmission File Run Times**

Interval ( $\text{cm}^{-1}$ )	Run Times (seconds):
13123 to 13167	35
13123 to 13167	31
13123 to 13167	36
13123 to 13167	34
13123 to 13167	36
13123 to 13167	36

On average, the second script took  $35 \text{ seconds} \pm 2 \text{ seconds}$  to compute the transmission. The reason for the longer than normal run times (e.g. LBLRTM takes under a second to compute transmission over this interval), is due to the time it takes Matlab to load the  $k(g)$  database, and check the values with the user's previous given path length and wavelength domain. For a series of six consecutive runs, the following transmission calculation times were recorded (excluding any user input, as well as the time needed to load the  $k(g)$  database).

**Table 6. Correlated-k Transmission Computation Times**

Interval (cm <sup>-1</sup> )	Run Times (seconds):
13123 to 13167	0.000524
13123 to 13167	0.000395
13123 to 13167	0.000615
13123 to 13167	0.000397
13123 to 13167	0.000433
13123 to 13167	0.000394

The average time needed to compute the transmittance, after importing the k(g) values, is  $4.597 \times 10^{-4}$  seconds.

As was mentioned in the previous Correlated-k section, in order to compare the Correlated-k transmission algorithm to LEEDR, LEEDR was run under two different circumstances. The first case attempted to obtain a similar amount of accuracy, with respect to the Correlated-k script. In order to obtain the 165 LEEDR transmission values over the 13123 cm<sup>-1</sup> to 13167 cm<sup>-1</sup> interval, the following times were recorded from LEEDR:

**Table 7. LEEDR Run Times for Comparable Transmission Resolution to Correlated-k**

Interval (cm <sup>-1</sup> )	Run Time:
13123 to 13167	6 minutes 37 seconds
13123 to 13167	6 minutes 59 seconds
13123 to 13167	7 minutes 4 seconds
13123 to 13167	7 minutes 1 seconds
13123 to 13167	7 minutes 4 seconds
13123 to 13167	7 minutes 16 seconds

The average run time for this case was 7 minutes 10 seconds, with a standard deviation of 15 seconds. In conclusion, in order to retain the same amount of accuracy as the Correlated-k, one would have to wait about 6 minutes 35 seconds longer for LEEDR to compute the transmission.

The other case that was presented in the previous section was a LEEDR transmission case which took the same order of time to compute as the Correlated-k script. Calculation times for this case were observed to be the following:

**Table 8. LEEDR Run Times Used to Display Transmission Accuracy Loss to Correlated-k**

Interval (cm <sup>-1</sup> )	Run Time (seconds):
13123 to 13167	48
13123 to 13167	48
13123 to 13167	48
13123 to 13167	48
13123 to 13167	48
13123 to 13167	48

The average run time in this case was 48 seconds. However, what is ultimately shown (through Table 7 and Figure 18) is that for a LEEDR run time comparable to the Correlated-k script, accuracy is sacrificed. For a 48 second LEEDR run time, one obtains 10 LEEDR transmission points, whereas the Correlated-k script is able to describe the interval with 11 transmission points.

## **V. Conclusions and Recommendations**

### **Overview**

This chapter is divided into two sections. The first section provides a conclusion of the research results presented in this paper for the user-defined Ground Level tab, as well as the Correlated-k algorithm. Subsequently, a section entitled Recommendations for Future Research discusses the modifications that need to be made to the Correlated-k algorithm, as seen by the author.

### **User-Defined Ground Level Input Tab**

In summary, the user-defined Ground Level tab in LEEDR enables the user to redefine several ground level values, to more accurately model upper air conditions. As is shown in Figure 10, a comparison of upper air sounding data from a nearby location to data from an ExPERT site, the GUI-modified values for boundary layer pressure, temperature, dewpoint, and relative humidity more closely resemble the upper air data, than the default LEEDR values. Furthermore, the LEEDR ground level GUI predicts very well the height of the boundary layer (which in Figure 10 was 1000 m for the LEEDR data, and 1031 m for the upper air sounding) and the temperature variation within it. After testing the accuracy of these values, the modified LEEDR program with the user-defined Ground Level tab will aid in SensorCAD model development at the Space Dynamics Laboratory at Utah State University.

### **Correlated-k**

The Correlated-k scripts provide a means of calculating the transmission in a much faster manner, while retaining some of the accuracy LBL calculations. On average, the Correlated-k scripts enable the user to calculate transmission from 13123  $\text{cm}^{-1}$  to

13167  $\text{cm}^{-1}$  over a 1 km vertical path length on average, 6 minutes 35 seconds faster than LEEDR. Running LEEDR for the same amount of time as the Correlated-k scripts would result in a drastic loss of accuracy. Importantly, the Correlated-k implemented in this research offers the LEEDR user a capability for fast, near-continuous consideration of each spectral band of interest when calculating transmission and/or extinction. This will enable future LEEDR path radiance calculations.

The transmission calculated from the Correlated-k scripts proved to be accurate when compared to the running means of LEEDR's transmission. However, when compared to the Modtran radiative transfer program in Plexus under a similar resolution, minor differences were noted over the current domain of the Correlated-k algorithm. These disparities are likely due to the different HITRAN databases that were utilized for each method. The average transmittance calculated from Plexus over the interval, 13123  $\text{cm}^{-1}$  to 13167  $\text{cm}^{-1}$ , was 0.683. The Correlated-k method, on the other hand, computed an average transmittance of 0.677. While these differences are small, future research (which will be suggested in the following section) is needed in implementing smaller band intervals and other inhomogeneous atmosphere techniques to achieve higher accuracy in the Correlated-k transmission values.

### **Recommendations for Future Research**

The calculation time of the Correlated-k script, as it stands, is an improvement over the LBL calculation algorithm currently incorporated into LEEDR, for a user-defined domain interval. The series of Matlab scripts enable the user to compute an accurate depiction of the transmission over a certain interval, in a homogeneous



atmosphere. Before extrapolating this method to nonhomogeneous atmospheres however, the accuracy of the Correlated-k transmission values needs to be improved.

The differences between the Correlated-k method and Plexus transmission values is believed to be due to the number of extinction points analyzed throughout a  $4 \text{ cm}^{-1}$  interval. For this project, 100 points were utilized. As was shown in Figures 11-12 at the beginning of the Results and Analysis section, 100 extinction points resulted in several bins without an extinction coefficient. Thus, the next logical step for the Correlated-k algorithm would be to increase the number of extinction coefficients per interval. In theory, as the amount of extinction points are increased, coefficients would begin to fill out different bins, and a better defined  $g$  value would be obtained. Thus, future research will have to determine the appropriate amount of extinction points to achieve accurate Correlated-k transmission values.

## Appendix

### Extinction Coefficient Database Source Code

```
%% Purpose
% File to read in LEEDR k vs. frequency values and write them to the
appropriate
% database.

clc; clear;
%% Variables
sheetNum = ['C' 'D' 'E' 'F' 'G' 'H' 'I'];
tol = 1e6;
newHeader = {'Frequency (Hz)' ' Wavelength (m)' ' Wavelength (um)' '
Wavelength (mm)' ' k_1km      '...
            ' k_2km      ' ' k_3km      ' ' k_4km      ' ' k_5km      ' '
k_6km      ' ' k_7km      ' ' k_8km      '};
firstCell = 0;
lastCell = 0;
newDataV = 'n';

%% User Input
% SELECT DATABASE.
[databaseFile,databasePath] = uigetfile({'*.txt'; '*.xls'}, 'Absorption
Co Database', 'L:\Students\10M\Ranney\Data');
if(isequal(databaseFile,0) || isequal(databasePath,0))
    newDataV = input('Create new database (enter y or n)? : ', 's');
    if(strcmp(newDataV, 'y'))
        [newFile,newPath] = uiputfile({'*.txt'; '*.xls'}, 'Select Name
and Path of New Database', 'L:\Students\10M\Ranney\Data'); % Can save
file as any type extention (.xls or .txt is default).
        if(isequal(newFile,0))
            disp('Terminating Program');
            return;
        end
    else
        disp('Terminating Program');
        return;
    end
else
    disp(['Extinction coefficient database: ',
fullfile(databasePath,databaseFile)]);
    oldData = dlmread(fullfile(databasePath,databaseFile), '', 1, 0);
    oldData(:,end) = [];
    disp(['Extinction Database has the following domain (cm-1): ['
num2str(round(inv(oldData(1,2).*100))) ' , '
num2str(round(inv(oldData(end,2).*100))) ' ]']');
    disp(['Extinction Database has ' num2str(size(oldData,1)) ' points
in the previously displayed domain']);
end

counter = 1;
% SELECT LEEDR FILE.
multiOption = 'off';
```

```

[leedrPlots,leedrPath] = uigetfile('*.fig','K vs. Frequency
Plot','L:\Students\10M\Ranney\Data','MultiSelect',multiOption);
if(isequal(leedrPlots,0) || isequal(leedrPath,0))
    disp('Terminating Program');
    return;
else
    disp('LEEDR absorption file: ');
    disp(fullfile(leedrPath,leedrPlots));
end

%% Extract Data From Plot
openfig(fullfile(leedrPath,leedrPlots));
freq = get(get(gca,'Children'),'xData');
kValues = get(get(gca,'Children'),'yData');
pathLength = str2double(input('Enter path length (km): ','s'));
res = input('Enter resolution (e.g. 1um,2cm-1,4cm-1,30cm-1): ','s');
if(strcmp(res,'4cm-1'))
    tolL = 1e10;
    tolU = 1e10;
else
    tol = 1e6;
end

%% Write To Tab-Delimited
if(strcmp(newDataV,'y'))
    databaseFile = newFile;
    databasePath = newPath;
end

if(strcmp(newDataV,'y'))
    absCoVars = zeros(length(newHeader),length(freq));
    absCoVars(1,:) = freq(:);
    absCoVars(2,:) = (3e8)./freq(:);
    absCoVars(3,:) = ((3e8)./freq(:)).*1e6;
    absCoVars(4,:) = ((3e8)./freq(:)).*1000;
    absCoVars(pathLength+4,:) = kValues(:);
    absCoVars = sortrows(absCoVars',1)';

    if(strcmp(databaseFile(end-3:end),'.xls'))

xlswrite(fullfile(databasePath,databaseFile),newHeader,region,'A1');

xlswrite(fullfile(databasePath,databaseFile),transpose(absCoVars),region,
'A2');
        else
            fid = fopen(fullfile(databasePath,databaseFile),'w');
            fprintf(fid,'%s',cell2mat(newHeader));
            fprintf(fid,'\r\n');
            fprintf(fid,'% -14.6g % -14.6g % -15.6g % -15.6g % -10.6g % -10.6g
% -10.6g % -10.6g % -10.6g % -10.6g % -10.6g % -10.6g \r\n',absCoVars);
            fclose(fid);
        end
    else
        newDataA = zeros(size(oldData,1)+length(freq),length(newHeader));
        newDataA(1:length(freq),1) = fliplr(freq);

```

```

newDataA(1:length(freq),2) = (3e8)./fliplr(freq);
newDataA(1:length(freq),3) = (3e8./fliplr(freq)).*1e6;
newDataA(1:length(freq),4) = (3e8./fliplr(freq)).*1000;
newDataA(1:length(freq),4+pathLength) = fliplr(kValues);
newDataA(length(freq)+1:end,:) = oldData(:,:);

cells = zeros(2,1);
for i=length(freq)+1:size(newDataA,1)
    if(abs(newDataA(1,1)-newDataA(i,1)) < tolL)
        cells(1) = i;
        tolL = abs(newDataA(1,1)-newDataA(i,1));
    elseif(abs(newDataA(length(freq),1)-newDataA(i,1)) <= tolU)
        cells(2) = i;
        tolU = abs(newDataA(length(freq),1)-newDataA(i,1));
    end
end

if((cells(2)-cells(1)+1) == size(oldData,1)) % new data is in same
domain as old data.
    disp('HERE1');
    newDataA(length(freq)+1:end,4+pathLength) = fliplr(kValues);
    newDataA(1:length(freq),:) = [];
elseif(isequal(cells(1),0) && isequal(cells(2),length(freq)+1)) %
new data resides before old data but has boundary issue.
    disp('HERE2');
    newDataA(length(freq)+1,4+pathLength) =
newDataA(length(freq),4+pathLength);
    newDataA(length(freq),:) = [];
elseif(isequal(cells(2),0) && isequal(cells(1),size(newDataA,1))) %
new data resides after old data but has boundary issue.
    disp('HERE3');
    newDataA(end,4+pathLength) = newDataA(1,4+pathLength);
    newDataA(1,:) = [];
    newDataA = sortrows(newDataA,1);
else % new data is somewhere within old data domain.
    disp('HERE4');
    newDataA(cells(1):cells(2),4+pathLength) = fliplr(kValues);
    newDataA(1:length(freq),:) = [];
end

fid = fopen(fullfile(databasePath,databaseFile),'w');
fprintf(fid,'%s',cell2mat(newHeader));
fprintf(fid,'\r\n');
fprintf(fid,'% -14.6g % -14.6g % -15.6g % -15.6g % -10.6g % -10.6g % -
10.6g % -10.6g % -10.6g % -10.6g % -10.6g % -10.6g \r\n',newDataA');
fclose(fid);
end

```

## Correlated-k Source Code

```
%% Purpose
% Creates expFit Database or computes transmission for the selected
region.

% Function:
% -Reads in absorption coefficient database from user (k vs.
% frequency).
% -Based on whether user supplies absorption database, script
prompts user
% for exponential fit database.
% -If user supplies absorption coefficient database and
% exponential fit database,
% -If user's wavelength interval and/or path length
doesn't
% coincide with exponential database, new exponential
data is
% appended.
% -Otherwise, transmission is computed.
% -If user supplies only absorption database,
% -Script checks user's wavelength interval and path
length
% to make sure it matches with absorption database, and
% subsequently adds the exponential fits from the
Correlated-k
% binning method to a new exponential fit database.
% -If user only supplies exponential database,
% -Scripts checks user wavelength interval and path
length to
% make sure it coincides with exponential database. If
% user-defined input is found in database, script
computes
% transmittance.

clc; clear;
tic
%% Input From User
[absFile,absPath] = uigetfile('*.txt', 'Select the Absorption
Database', 'L:\Students\10M\Ranney\Data');
if isequal(absFile,0) || isequal(absPath,0)
    disp('No Absorption Database Selected');
else
    disp(['Absorption Database: ', fullfile(absPath,absFile)]);
    absData = dlmread(fullfile(absPath,absFile),'',1,0);
    absData(:,end) = []; % dlmread reads in blank column after k_8
    (return character after last write statement?).
    disp(['Absorption Database has the following domain (cm-1): ['
num2str(round(inv(absData(1,2).*100))) ', '
num2str(round(inv(absData(end,2).*100))) ']]');
    disp(['Absorption Database has ' num2str(size(absData,1)) ' files
in the previously displayed domain']);
    absData = sortrows(absData,2); % flips data in terms of increasing
wavelength.
end
```

```

[kgFile,kgPath] = uigetfile('*.txt','Select k(g)
Database','L:\Students\10M\Ranney\Data');
if isequal(kgFile,0) || isequal(kgPath,0)
    if(~exist('absData','var'))
        disp('No k(g) Database Selected');
        disp('Terminating Program');
        return;
    else
        disp('No k(g) Database Selected');
    end
else
    disp(['k(g) Database: ' fullfile(kgPath,kgFile)]);
    kgFitData = dlmread(fullfile(kgPath,kgFile),'',0,0);
    kgFitData(:,end) = [];
    kgFitData(:,1) = 3e8./kgFitData(:,1);
    kgFitData = sortrows(kgFitData,1);
    disp(['Wavelength domain of files currently in database: ['
num2str(kgFitData(1,1),'%-3.5e') ',' num2str(kgFitData(end,1),'%-3.5e')
']']);
    disp(['Number of points in domain: '
num2str(round(size(kgFitData,1)/2))]');
end
lowerPath = input('Enter lower path length (m): '); % Input coincides
with LEEDR.
upperPath = input('Enter upper path length (m): ');
lowerWave = input('Enter lower wavelength bound (m) (5 decimal place
accuracy): ');
upperWave = input('Enter upper wavelength bound (m) (5 decimal place
accuracy): ');
waveRes = input('Enter wavelength domain resolution (e.g. 1cm-1,4cm-
1,lum): ','s');
if(strcmp(waveRes,'4cm-1'))
    tol = 1e-11;
else
    tol = 1e-8;
end
numBins = 16;

%% Checking user input.
corrKBool = 0;
if(lowerWave>=upperWave || lowerPath>=upperPath)
    disp('Bad Wavelength/Path Bounds');
    return;
end
if(exist('kgFitData','var'))
    [corrKBool,waveInt] =
kgCheck(unique(kgFitData(:,1),'first'),corrKBool,lowerWave,upperWave,to
l);
else
    corrKBool = 1;
end
if(exist('absData','var'))
    if(lowerWave < absData(1,2) || upperWave > absData(end,2))
        disp('User defined wavelength is outside absorption database');
        return;
    end
end

```

```

    end
    if(absData(length(find((absData(:,2)-(absData(2,2)-
absData(1,2))./2)<=lowerWave)),(upperPath-lowerPath)./1000)+4) == 0)
        disp('No absorption data exists for user-defined path length');
        return;
    end
end

%% Correlated-k Binning Method
if(corrKBool)
    if(~exist('absData','var'))
        disp('Cannot perform Correlated-k method. No absorption
database supplied');
        return;
    end

    lowerCell = length(find(absData(:,2)<=lowerWave));
    upperCell = size(absData,1)-length(find(absData(:,2)>upperWave));
    if(upperCell>size(absData,1))
        upperCell = size(absData,1);
    end

    expFitRes = round((round(inv(lowerWave*100))-
round(inv(upperWave*100)))/4); % Determining number of 4cm-1 intervals.
    gXCounter = zeros(numBins+1,1);
    yIntervals = zeros(numBins+1,1);
    gSumMat = zeros(numBins);

    newBoundWave =
linspace(absData(lowerCell,2),absData(upperCell,2),expFitRes+1)';
    disp(['Resolution is set at: ' num2str((newBoundWave(2)-
newBoundWave(1)).*1e9) ' nm']);

    % Determines which data points fall in newly defined wavelength
% boundary
    cellBoundary = zeros(expFitRes+1,1);
    absCo = zeros(upperCell-lowerCell+1,1);
    cellBoundary(1) = 1;
    for i=2:length(cellBoundary)-1
        cellBoundary(i) = cellBoundary(i-1)+length(find(newBoundWave(i-
1) < absData(lowerCell:upperCell,2) & newBoundWave(i) >
absData(lowerCell:upperCell,2)));
    end
    cellBoundary(end) = upperCell-lowerCell+1;
    absCo(:) = absData(lowerCell:upperCell,((upperPath-
lowerPath)./1000)+4);

    % Allocate arrays for kgFit data
    if(isequal(kgFile,0))
        kgOutputData = zeros(2*expFitRes,numBins+2);
    else
        kgOutputData = zeros(2*expFitRes+size(kgFitData,1),numBins+2);
        kgOutputData(2*expFitRes+1:end,:) = kgFitData;
    end
end

```

```

kgOutputData(1:expFitRes,1) = newBoundWave(1:end-
1)+(newBoundWave(2)-newBoundWave(1))./2;
kgOutputData(expFitRes+1:2*expFitRes,1) = newBoundWave(1:end-
1)+(newBoundWave(2)-newBoundWave(1))./2;
kgOutputData(1:2*expFitRes,:) =
sortrows(kgOutputData(1:2*expFitRes,:),1);

% Correlated-k Binning Method
for i=1:expFitRes
    if(i == 1)
        yMin = min(absCo(cellBoundary(i):cellBoundary(i+1)));
        yMax = max(absCo(cellBoundary(i):cellBoundary(i+1)));
    else
        yMin = min(absCo(cellBoundary(i)+1:cellBoundary(i+1)));
        yMax = max(absCo(cellBoundary(i)+1:cellBoundary(i+1)));
    end

    yIntervals(1:end) = linspace(yMin,yMax,numBins+1)';
    gXCounter(1:end) =
histc(absCo(cellBoundary(i):cellBoundary(i+1)),yIntervals(:))';
    gXCounter(end-1) = gXCounter(end-1)+gXCounter(end);
% Creates k values that are in the middle of the intervals.
    kgOutputData(i+i-1,2) = 0;
    kgOutputData(i+i-1,3:end) = yIntervals(1:end-
1)+(yIntervals(2:end)-yIntervals(1:end-1))./2;

% Calculating k(g). Puts bin summations in lower triangular matrix.
    for j=1:numBins
        gSumMat(j,1:end) = gXCounter(1:end-1)';
    end
    gXCounter(1:end-1) = sum(tril(gSumMat,0),2)';

% Creates g points by dividing sum
    kgOutputData(2*i,2) = 0;
    kgOutputData(2*i,3:end) = gXCounter(1:end-1)./gXCounter(end-1);
% Removed transpose.
end

% Deleting duplicate data assuming database contains the same
% resolution.
if(~isequal(kgFile,0))
    cells = zeros(1,2);
    tol = (newBoundWave(2)-newBoundWave(1))./2;
    counter = 0;
    for i=2*expFitRes+1:(2*expFitRes+1)+round(size(kgFitData,1)./2)
        if(abs(kgOutputData(1,1)-kgOutputData(i+counter,1)) < tol)
            cells(1) = i+counter;
        elseif(abs(kgOutputData(2*expFitRes,1)-
kgOutputData(i+counter,1)) < tol)
            cells(2) = i+counter;
        end
        counter = counter+1;
    end
end

```



```

        if(isequal(cells(1),0) && isequal(cells(2),2*expFitRes+1)) %
new data has domain that starts after old data, with overlapping
boundary.
            disp('Here2');
            kgOutputData(2*expFitRes-1,:) =
kgOutputData(2*expFitRes+1,:);
            kgOutputData(2*expFitRes,:) =
kgOutputData(2*expFitRes+2,:);
            kgOutputData(2*expFitRes+1,:) = [];
            kgOutputData(2*expFitRes+2,:) = [];
            elseif(isequal(cells(2),0) &&
isequal(cells(1),size(kgOutputData,1)-1)) % new data has domain that
starts before old data, with overlapping boundary.
                disp('Here3');
                kgOutputData(1,:) = kgOutputData(size(kgOutputData,1)-1,:);
                kgOutputData(2,:) = kgOutputData(size(kgOutputData,1),:);
                kgOutputData(size(kgOutputData,1)-1,:) = [];
                kgOutputData(size(kgOutputData,1),:) = [];
                else % new data is outside old frequency range.
                    kgOutputData = sortrows(kgOutputData,1);
                end
            kgOutputData = sortrows(expOutputData,1);
        end
    toc
    %% Writing Exponential Fits/K(g) Points to Database
    if(isequal(kgFile,0))
        [kgOutputPath,kgOutputFile] = uiputfile('*.txt','Enter Name for
kgFit Database','L:\Students\10M\Raney\Data');
        if(isequal(kgOutputFile,0))
            disp('No kgFit Database Selected');
            return;
        else
            disp(['kgFit Database: '
fullfile(kgOutputPath,kgOutputFile)]);
        end
    else
        disp(['kgFit Database: ' fullfile(kgPath,kgFile)]);
        kgOutputFile = kgFile;
        kgOutputPath = kgPath;
    end

    % K(g) data not currently incorporated into transmission.
    kgFid = fopen(fullfile(kgOutputPath,kgOutputFile),'w');
    kgOutputData(:,1) = 3e8./kgOutputData(:,1); % Transform to
frequency
    kgOutputData = sortrows(kgOutputData,1);
    fprintf(kgFid,'% -13.5e % -10.6g % -10.6g % -10.6g % -10.6g % -10.6g % -
10.6g % -10.6g % -10.6g % -10.6g % -10.6g % -10.6g % -10.6g % -10.6g % -
10.6g % -10.6g % -10.6g \r\n',kgOutputData');
    fclose(kgFid);

    %% Calculating Transmission
    else
        gValues = zeros(1,round(size(kgFitData,1)./2));
        gValues(1,:) = unique(kgFitData(:,1),'first');

```

```

kgFitTrans = zeros((length(gValues)-
length(find(gValues(:)>(upperWave))))-
length(find(gValues(:)<=(lowerWave)))+1,1);

% Loading Leedr Transmission Plot
[leedrFile,leedrPath] = uigetfile('*.fig','Leedr Transmission File
in Frequency Domain','L:\Students\10M\Ranney\Data');
if(isequal(leedrFile,0) || isequal(leedrPath,0))
    disp('No LEEDR transmission file selected');
else
    disp(['LEEDR transmission file: ',
fullfile(leedrPath,leedrFile)]);
    openfig(fullfile(leedrPath,leedrFile));
    leedrTrans = get(get(gca,'Children'),'yData');
    leedrWave = 3e8./get(get(gca,'Children'),'xData'); % Assuming
Frequency domain.
    leedrWave = sortrows(leedrWave,1);

    leedrTrans(leedrWave>upperWave) = [];
    leedrWave(leedrWave>upperWave) = [];
    leedrTrans(leedrWave<lowerWave) = [];
    leedrWave(leedrWave<lowerWave) = [];
end

massPathNum = (upperPath-lowerPath)/1000;
for
i=length(find(gValues(:)<=(lowerWave+waveInt))):(length(gValues)-
length(find(gValues(:)>(upperWave))))-
length(find(gValues(:)<=(lowerWave)))+1
    for j=3:numBins+2
        kgFitTrans(i) = kgFitTrans(i)+((abs(exp(-kgFitData((i+i-
1),j-1))-exp(-kgFitData((i+i-1),j))).*massPathNum)*(kgFitData(2*i,j)-
kgFitData(2*i,j-1)))./2;
        if(exp(-kgFitData((i+i-1),j))>exp(-kgFitData((i+i-1),j-1)))
            kgFitTrans(i) = kgFitTrans(i)+exp(-kgFitData((i+i-1),j-
1)).*massPathNum).*(kgFitData(2*i,j)-kgFitData(2*i,j-1));
        else
            kgFitTrans(i) = kgFitTrans(i)+exp(-kgFitData((i+i-
1),j)).*massPathNum).*(kgFitData(2*i,j)-kgFitData(2*i,j-1));
        end
    end
end
end
toc
%% Plotting the Transmission Over the User-Specified Interval
tol = 1e-8;
if(lowerWave <= 50e-6 || abs(lowerWave-50e-6) < tol)
    if(~isequal(leedrFile,0))
        figure
        plot(leedrWave.*1e6,leedrTrans,'b-'); % Assuming meter
domain.

        hold on;
        plot(gValues.*1e6,kgFitTrans,'r-');
        hold off;
        legend('LEEDR','Correlated-k');
    else

```

```

        plot(gValues.*1e6,kgFitTrans,'r-');
        legend('Correlated-k');
    end
    xlabel('Wavelength (\mum)');
elseif(lowerWave > 50e-6)
    if(~isequal(leedrFile,0))
        figure
        plot(leedrWave.*1000,leedrTrans,'b-');
        hold on;
        plot(gValues.*1000,kgFitTrans,'r-');
        hold off;
        legend('LEEDR','Correlated-k');
    else
        plot(gValues.*1000,kgFitTrans,'r-');
        legend('Correlated-k');
    end
    xlabel('Wavelength (mm)');
end
ylabel('Transmission');
title('Transmission vs. Wavelength');
end

```

### kgCheck Function (Correlated-k)

```

function [corrKBool,waveInt] =
kgCheck(gValues,corrKBool,lowerWave,upperWave,tol)
    if(size(gValues,1) > 1)
        waveInt = abs(gValues(2)-gValues(1))/2;
    else
        waveInt = abs(gValues(1)-inv((inv(gValues(1)*100)+2))/100); %
Assumes a 4cm-1 interval
    end
    if(lowerWave<(gValues(1)-waveInt)) % LowerWave exists outside
exponential database
        if(abs(lowerWave-(gValues(1)-waveInt))<tol) % LowerWave is
close enough to lower bound of exponential database. Current tolerance
is 10.^-13 (lum resolution).
            corrKBool = 0;
        else
            corrKBool = 1;
            disp('User defined lower wavelength is outside kgFit
database');
        end
    end
    if(upperWave>(gValues(end)+waveInt)) % UpperWave exists outside
exponential database
        if(abs(upperWave-(gValues(end)+waveInt))<tol) % UpperWave is
close enough to lower bound of exponential database
            corrKBool = 0;
        else
            corrKBool = 1;
            disp('User defined upper wavelength is outside kgFit
database');
        end
    end
end end

```

## Bibliography

- [1] (2009) Modtran5: Narrow band model atmospheric radiative transfer code. [Online].  
HYPERLINK "http://www.modtran.org/index.html" <http://www.modtran.org/index.html>
- [2] R. R. Beland, *Propagation Through Atmospheric Optical Turbulence*, 2nd ed., F. G. Smith, Ed. Hanscom AFB, Massachusetts: OptiMetrics Incorporated.
- [3] M. -D. Chou and L. Kouvaris, "Monochromatic Calculations of Atmospheric Radiative Transfer due to Molecular Line Absorption," vol. 91, no. D3, 1986.
- [4] G. A. D'Almeida, P. Koepke, and E. P. Shettle, *Atmospheric Aerosols: Global Climatology and Radiative Characteristics*. Hampton: A. Deepak Publishing, 1991.
- [5] S. T. Fiorino, R. J. Bartell, M. J. Krizo, and S. J. Cusumano, "Propagation Variability Assessments of Ship Defense HEL and HPM Performance in Worldwide Maritime Boundary Layer Environments at Wavelengths of 1.0642 $\mu$ m, 2.141 $\mu$ m, 3.16mm, and 12.2cm," in , vol. 6951, Wright Patterson AFB, 2008.
- [6] S. T. Fiorino, et al., "A First Principles Atmospheric Propagation & Characterization Tool: the Laser Environmental Effects Definition and Reference (LEEDR)," in , vol. 6878, Wright Patterson AFB, 2008.
- [7] S. G. Gathman, A. M. J. van Eijk, and L. H. Cohen, "Characterizing Large Aerosols in the Lowest Level of the Marine Atmosphere," in , San Diego, 1998.
- [8] Space Dynamics Laboratory. (2009, Jun.) UARC Five Year Comprehensive Review. Powerpoint.
- [9] K. N. Liou, *An Introduction to Atmospheric Radiation*. San Diego: Academic Press, 2002.
- [10] K. N. Liou and Q. Fu, "On the Correlated-k k-Distribution Method for Radiative Transfer in Nonhomogeneous Atmospheres," vol. 49, no. 22, 1992.
- [11] G. W. Petty, *A First Course in Atmospheric Radiation*. Madison: Sundog Publishing, 2006.
- [12] D. Schlapfer, "MODO: An Interface to Modtran for the Simulation of Imaging Spectrometry At-Sensor Signals," in *Tenth Jet Propulsion Laboratory Airborne Earth Science Workshop*, Pasadena, 2001, pp. 343-350.
- [13] G. Shi, X. Na, W. Biao, D. Tie, and Z. Jianqi, "An improved treatment of overlapping absorption bands based on the correlated k distribution model for thermal infrared

radiative transfer calculations," vol. 110, no. 8, 2009.

- [14] Navy SPAWAR. (2009, Jun.) Generating an Accurate Vertical Aerosol Profile. Powerpoint.
- [15] National Oceanic and Atmospheric Administration. (2009, Mar.) NCDC: Unedited Local Climatological Data. [Online]. HYPERLINK "<http://cdo.ncdc.noaa.gov/ulcd/ULCD>"  
<http://cdo.ncdc.noaa.gov/ulcd/ULCD>
- [16] Atmospheric and Environmental Research Inc. (2010, Jan.) LBLRTM (Line-By-Line Radiative Transfer Model). [Online]. HYPERLINK "<http://rtweb.aer.com/lblrtm.html>"  
<http://rtweb.aer.com/lblrtm.html>
- [17] C. F. Bohren, *Clouds in a Glass of Beer*. New York: John Wiley & Sons, Inc., 1987.
- [18] University of Wyoming: Department of Atmospheric Science. [Online]. HYPERLINK "<http://weather.uwyo.edu/upperair/sounding.html>"  
<http://weather.uwyo.edu/upperair/sounding.html>
- [19] National Ocean and Atmospheric Administration. [Online]. HYPERLINK "<http://www.weather.gov/climate/index.php?wfo=iln>"  
<http://www.weather.gov/climate/index.php?wfo=iln>
- [20] R. J. List, *Smithsonian Meteorological Tables*. Washington, 1949.
- [21] S. T. Fiorino. (2009) Water Vapor in the Air. PowerPoint.
- [22] J. M. Wallace and P. V. Hobbs, *Atmospheric Science: An Introductory Survey*. Burlington: Academic Press, 2006.
- [23] (2009, Dec.) The HITRAN Database. [Online]. HYPERLINK "<http://www.cfa.harvard.edu/hitran/>" <http://www.cfa.harvard.edu/hitran/>
- [24] L. S. Rothman et al. (2003) The Hitran molecular spectroscopic database: edition of 2000 including updates through 2001. [Online]. HYPERLINK "<http://www.cfa.harvard.edu/hitran/>" <http://www.cfa.harvard.edu/hitran/>

REPORT DOCUMENTATION PAGE			Form Approved OMB No. 074-0188		
<p>The public reporting burden for this collection of information is estimated to average 1 hour per response, including the time for reviewing instructions, searching existing data sources, gathering and maintaining the data needed, and completing and reviewing the collection of information. Send comments regarding this burden estimate or any other aspect of the collection of information, including suggestions for reducing this burden to Department of Defense, Washington Headquarters Services, Directorate for Information Operations and Reports (0704-0188), 1215 Jefferson Davis Highway, Suite 1204, Arlington, VA 22202-4302. Respondents should be aware that notwithstanding any other provision of law, no person shall be subject to a penalty for failing to comply with a collection of information if it does not display a currently valid OMB control number.</p> <p><b>PLEASE DO NOT RETURN YOUR FORM TO THE ABOVE ADDRESS.</b></p>					
<b>1. REPORT DATE (DD-MM-YYYY)</b> 17-06-2010		<b>2. REPORT TYPE</b> Master's Thesis		<b>3. DATES COVERED (From – To)</b> June 2009 – June 2010	
<b>4. TITLE AND SUBTITLE</b>  Realistic Vertical Atmospheric Profiles and Effects from Limited Surface Observations			<b>5a. CONTRACT NUMBER</b>		
			<b>5b. GRANT NUMBER</b>		
<b>6. AUTHOR(S)</b>  Ranney, Dane P., Civ, USAF			<b>5c. PROGRAM ELEMENT NUMBER</b>		
			<b>5d. PROJECT NUMBER</b>		
<b>7. PERFORMING ORGANIZATION NAMES(S) AND ADDRESS(S)</b> Air Force Institute of Technology Graduate School of Engineering and Management (AFIT/EN) 2950 Hobson Way WPAFB OH 45433-7765			<b>5e. TASK NUMBER</b>		
			<b>5f. WORK UNIT NUMBER</b>		
<b>8. PERFORMING ORGANIZATION REPORT NUMBER</b>  AFIT/GAP/ENP/10-M12			<b>8. PERFORMING ORGANIZATION REPORT NUMBER</b>		
			<b>10. SPONSOR/MONITOR'S ACRONYM(S)</b> SDL		
<b>9. SPONSORING/MONITORING AGENCY NAME(S) AND ADDRESS(ES)</b> Space Dynamics Laboratory 1695 North Research Park Way North Logan, UT 85341 Mr. Justin Tidwell (435) 797-5825			<b>11. SPONSOR/MONITOR'S REPORT NUMBER(S)</b>		
			<b>11. SPONSOR/MONITOR'S REPORT NUMBER(S)</b>		
<b>12. DISTRIBUTION/AVAILABILITY STATEMENT</b>  APPROVED FOR PUBLIC RELEASE; DISTRIBUTION UNLIMITED.					
<b>13. SUPPLEMENTARY NOTES</b>					
<b>14. ABSTRACT</b> <p>The ability to accurately describe the atmospheric conditions around us is not only important to the Air Force, but to anyone involved in signal propagation. The programs currently utilized to describe the atmosphere take into account a variety of measures. The LEEDR (Laser Environmental Effects Definition and Reference) program in particular, allows the user to select a location, aerosol and molecular effects model, numerous cloud and precipitation events, as well as other features. Even with the control that the user has, the output that the program provides can vary from actual conditions on a day to day basis. This is due to LEEDR's dependence on averaged climatological data. In order to make the output more specific for deterministic conditions, two additions to the LEEDR program have been proposed. The incorporation of calculated or measured ground level characteristics will allow the program to extrapolate data from scenario-specific anchor points, leading to a more realistic depiction of conditions below the boundary layer for the scenario of interest. After making this modification to the LEEDR program, differences were observed in several of the output variables throughout the boundary layer. Also, after interpolating sounding data from a location near the LEEDR site to model ground level conditions, LEEDR was able to more accurately model upper air measurements. In addition, a Correlated-k band model has been developed to augment the line-by-line LEEDR calculation in order to reduce the computation time required to describe atmospheric transmission bands of the spectrum. This allows the implementation of fast calculating path radiance computations. As a stand-alone module, the Correlated-k method is able to calculate transmission for the band interval studied, assuming a homogeneous atmosphere on average, 170% faster than the current transmission method in LEEDR.</p>					
<b>15. SUBJECT TERMS</b>  Correlated-k, LEEDR, Radiative Transfer					
<b>16. SECURITY CLASSIFICATION OF:</b>		<b>17. LIMITATION OF ABSTRACT</b>  UU	<b>18. NUMBER OF PAGES</b>  101	<b>19a. NAME OF RESPONSIBLE PERSON</b> Steven T. Fiorino, Civ (ENP)	
REPORT U	ABSTRACT U			<b>19b. TELEPHONE NUMBER (Include area code)</b> (937) 255-3636, ext 4506 (steven.fiorino@afit.edu)	

Standard Form 298 (Rev. 8-98)  
Prescribed by ANSI Std. Z39-18